© 2014. Published by The Company of Biologists Ltd | Development (2014) 141, 2313-2324 doi:10.1242/dev.108100

RESEARCH ARTICLE

Ligand-dependent Notch signaling strength orchestrates lateral induction and lateral inhibition in the developing inner ear

Jelena Petrovic[1,‡], Pau Formosa-Jordan[2,‡], Juan C. Luna-Escalante[2], Gina Abelló[1], Marta Ibañes[2,§], Joana Neves[1,*,§] and Fernando Giraldez[1,§]

ABSTRACT

During inner ear development, Notch exhibits two modes of operation: lateral induction, which is associated with prosensory specification, and lateral inhibition, which is involved in hair cell determination. These mechanisms depend respectively on two different ligands, jagged 1 (Jag1) and delta 1 (Dl1), that rely on a common signaling cascade initiated after Notch activation. In the chicken otocyst, expression of Jag1 and the Notch target Hey1 correlates well with lateral induction, whereas both Jag1 and Dl1 are expressed during lateral inhibition, as are Notch targets Hey1 and Hes5. Here, we show that Jag1 drives lower levels of Notch activity than Dl1, which results in the differential expression of Hey1 and Hes5. In addition, Jag1 interferes with the ability of Dl1 to elicit high levels of Notch activity. Modeling the sensory epithelium when the two ligands are expressed together shows that ligand regulation, differential signaling strength and ligand competition are crucial to allow the two modes of operation and for establishing the alternate pattern of hair cells and supporting cells. Jag1, while driving lateral induction on its own, facilitates patterning by lateral inhibition in the presence of Dl1. This novel behavior emerges from Jag1 acting as a competitive inhibitor of Dl1 for Notch signaling. Both modeling and experiments show that hair cell patterning is very robust. The model suggests that autoactivation of proneural factor Atoh1, upstream of Dl1, is a fundamental component for robustness. The results stress the importance of the levels of Notch signaling and ligand competition for Notch function.

KEY WORDS: Sensory development, Hair cells, Atoh1, Mathematical modeling, Systems biology, Signal competition

INTRODUCTION

Notch signaling plays a dual role during the sensory development of the inner ear, where it is required during early stages of prosensory specification and also for hair cell determination (Neves et al., 2013). The prosensory function of Notch relies on lateral induction, which is defined as the process by which a ligand-expressing cell stimulates those nearby to upregulate ligand expression, promoting ligand propagation and a coordinated cell behavior (Eddison et al., 2000). Hair cell determination results from lateral inhibition, whereby a ligand-expressing cell inhibits the expression of the ligand in the neighbors, thereby preventing them from adopting the same fate and generating a fine-grained cellular pattern (Bray, 2006). These two modes of operation rely, in each case, on the associated gene regulatory circuit. The prosensory function of Notch is mediated by the Notch ligand jagged 1 [Jag1; also known as serrate 1 (Ser1) in chick] (Eddison et al., 2000; Brooker et al., 2006; Kiernan et al., 2006; Daudet et al., 2007; Hartman et al., 2010; Pan et al., 2010; Neves et al., 2011). In the developing inner ear, *Jag1* induces its own expression in adjacent cells and the expression of prosensory genes such as *Sox2*, resulting in the homogenous commitment of otic progenitors to the prosensory fate (Neves et al., 2011). By contrast, hair cell determination is driven by the Notch ligand delta 1 [Dl1; also known as delta-like 1 (Dll1) in chick] (Haddon et al., 1998; Daudet and Lewis, 2005; Kiernan et al., 2005; Brooker et al., 2006). Dl1 expression is thought to be induced by the transcription factor Atoh1, which initiates hair cell development (Mulvaney and Dabdoub, 2012). Atoh1 activates its own transcription (Helms et al., 2000) and is inhibited by Notch signaling (Takebayashi et al., 2007; Doetzlhofer et al., 2009). Lateral inhibition between cells mediated by *Dl1* is resolved into a fine-grained pattern of hair and supporting cells (Collier et al., 1996). Notch target genes of the Hes family (Hairy and Enhancer of split paralogs) and Hes-related factors (Hesr, Hey/Herp genes) function as transcriptional repressors (Iso et al., 2003; Fischer and Gessler, 2007); they repress Atoh1 and are crucial for hair cell development (Zheng et al., 2000; Zine et al., 2001; Tateya et al., 2011; Du et al., 2013).

During the developmental window in which prosensory precursors transit to hair cell fate commitment, both Jag1 and Dl1 are expressed in the otic epithelium. This raises the question of how sensory precursors deal with the simultaneous presence of the two ligands, and how the final pattern is resolved. Lateral induction and lateral inhibition have been described as distinct circuits leading to specific cellular outputs of ligand propagation versus fine-grained patterning, respectively. Yet, there is no description of how these circuits cooperate and/or antagonize each other during development.

The present work shows that, in the chick inner ear, Jag1 induces weaker levels of Notch activity than Dl1, resulting in the differential expression of the target genes *Hey1* and *Hes5* as functional readouts. When both ligands signal together, competition arises and Jag1 decreases the overall signaling. Modeling indicates that, under such conditions, Jag1 operates as a partial agonist of Notch, effectively acting as a competitive inhibitor of Dl1/Notch signaling. In consequence, Jag1 inhibits its own expression in neighboring cells, thereby facilitating lateral inhibition and hair cell patterning. Experiments and modeling show that hair cell patterning is highly robust and that Jag1 biases, but does not determine, the supporting cell fate. The model attributes this robustness to Atoh1 autoactivation upstream of Dl1.

[1]Developmental Biology Unit, CEXS, Universitat Pompeu Fabra, Parc de Recerca Biomèdica de Barcelona (PRBB), 08003 Barcelona, Spain. [2]Departament d'Estructura i Constituents de la Matèria, Facultat de Física, Universitat de Barcelona, 08028 Barcelona, Spain.
*Present address: The Buck Institute, 8001 Redwood Boulevard, Novato, CA 94945-1400, USA.
‡These authors contributed equally to this work

§Authors for correspondence (mibanes@ub.edu; jneves@buckinstitute.org; fernando.giraldez@upf.edu)

Received 27 January 2014; Accepted 11 April 2014

Development (2014) 141, 2313-2324 doi:10.1242/dev.108100

RESULTS

Dl1 and Jag1 are associated with different Notch targets during ear development

Hes/Hey factors are well-known targets of Notch signaling and are required for inner ear development (Zheng et al., 2000; Zine et al., 2001; Hayashi et al., 2008; Li et al., 2008; Tateya et al., 2011). We asked whether there is a relationship between the expression of the ligands Dl1 and Jag1 and the different Hes/Hey genes. In the chicken inner ear, Jag1 is expressed during both prosensory and hair cell differentiation stages, whereas Dl1 is only expressed during the latter (Adam et al., 1998; Morrison et al., 1999; Cole et al., 2000). From several Hes and Hey genes screened, only *Hes5* and *Hey1* mapped to the sensory domains. Sensory development follows a dorsal-to-ventral sequence and, at the stage shown in Fig. 1A (E5), the dorsalmost patches (cristae and macula utricularis) had initiated differentiation, whereas the ventralmost domains (macula sacularis and basilar papilla) were still prosensory. This allows different developmental stages to be observed in a single specimen. *Hey1* was expressed along with Jag1 in the sensory epithelium, from the dorsalmost cristae to the maculae and the basilar papilla (pc, ms and bp in Fig. 1Aa-f). The expression of *Hes5* differed from that of *Hey1* and did not parallel Jag1. *Hes5* was expressed only in the dorsalmost patches (pc, ac and mu in Fig. 1Ag,p,q), but not in the ventral domains (ms and bp in Fig. 1Ah,i,r) that exhibited a strong Jag1 signal (Fig. 1Ab,c,l). Interestingly, *Hes5* expression matched well with that of *Dl1* (Fig. 1A, compare m,n with p,q).

The expression patterns of *Jag1*, *Dl1*, *Hes5* and *Hey1* genes during prosensory and hair cell determination are illustrated in Fig. 1B. During prosensory stages, Jag1 and *Hey1* showed a homogeneous cellular expression pattern (Fig. 1Ba,b), whereas during hair cell determination *Dl1* showed a speckled pattern similar to that of *Atoh1* expression in nascent hair cells (Fig. 1Bc,g,h). By contrast, *Jag1*, *Hey1* and *Hes5* were expressed in the basal layer that corresponds to supporting cells (Fig. 1Bd-f), complementary to the luminal layer occupied by MyoVIIa-positive hair cells (Fig. 1Bh).

These observations suggest that, throughout development, different Notch ligands result in the activation of different downstream genes. To test this, we analyzed the effects of Dl1 or Jag1 gain-of-function on *Hey1* and *Hes5* expression in the otic vesicle.

Dl1 and Jag1 differentially regulate *Hey1* and *Hes5*

The timecourse of *Hey1* and *Hes5* mRNA levels after human JAG1 (hJag1) or chick Dl1 (cDl1) electroporation is shown in Fig. 2A,B. *Hey1* was significantly induced by both ligands at all time points examined. *Hes5* was also induced by Dl1 (Fig. 2B), but only weakly by Jag1, and delayed with respect to *Hey1* (Fig. 2A). *Hey1* induction was always stronger than that of *Hes5* after Jag1 overexpression, whereas the effects of Dl1 on *Hey1* and *Hes5* were not significantly different after 6 h. This is illustrated by a comparison of the relative mRNA increase (fold increase) for each condition (Fig. 2C,D; supplementary material Fig. S1). In these experiments, the amount of transcribed hJag1 and cDl1 was checked to be equivalent (supplementary material Fig. S1Aa). The results suggest that *Hey1* and *Hes5* are differentially regulated by Jag1 and Dl1.

Given that both Dl1 and Jag1 activate the same signaling pathway, we sought possible explanations for their different actions on target genes. Since Notch1 is the only Notch receptor expressed in the inner ear of the chick embryo at the developmental stages under study (Adam et al., 1998; Abelló et al., 2007), the activation of different intracellular cascades for Dl1 and Jag1 is unlikely. One possible explanation is that the different ligands induce different strengths of Notch signal, which in turn result in different outputs. In the experiments that follow, we first explored whether different levels of active Notch differentially regulate Notch target genes and, second, whether Dl1 and Jag1 induce different levels of Notch activity.

Different levels of Notch activity result in the activation of different targets

We tested the effects of the loss and gain of function of Notch on *Hey1* and *Hes5* to then further analyze the quantitative relationship between Notch activity and target activation. We examined the expression of Notch ligands (Fig. 3A) and targets (Fig. 3B) after incubation with the γ-secretase inhibitor LY411575 (Ferjentsik et al., 2009). As expected from the different regulatory circuits (Notch inhibition or activation of the ligand), Notch blockade showed opposite effects on *Dl1* and *Jag1* (Fig. 3A). Also as expected for direct target genes, *Hey1* and *Hes5* expression was strongly repressed after Notch inhibition (Fig. 3B). Note that ∼20% of *Hey1* expression was refractory to Notch inhibition, suggesting the presence of alternative regulatory mechanisms.

To test whether differences in Notch signaling strength impact Notch target selection, we measured the expression of *Hey1* and *Hes5* with different concentrations of intracellular Notch [mouse Notch1 intracellular domain (mNICD1, or NICD)] (Fig. 3C; see supplementary material Fig. S2 for absolute mRNA levels). Low NICD (<0.1 µg/µl) induced *Hey1* but not *Hes5* expression, whereas intermediate and high NICD levels (1-2.5 µg/µl) induced both Notch targets, with a preference for *Hes5*. This indicates that the threshold for *Hey1* induction by NICD was lower than that for *Hes5*.

The different sensitivity of *Hey1* and *Hes5* to Notch signaling levels was further studied by overexpressing two hypomorphic *Notch1* gain-of-function constructs (L1601P and L1601PΔP) that harbor a mutation in the heterodimerization domain of the Notch1 receptor (HD mutation). The two constructs are less potent than the wild-type NICD, as evaluated by 4xCSL-luciferase reporter (Chiang et al., 2008). Electroporation of either construct induced *Hey1* but not *Hes5* (Fig. 3D). L1601P and L1601PΔP phenocopied low levels of NICD (0.01 and 0.1 µg/µl; Fig. 3D). These results reinforce the notion that low levels of Notch activity are sufficient to induce *Hey1* but not *Hes5* in the inner ear.

Different Notch ligands induce different levels of Notch activity

The possibility that Dl1 and Jag1 induce different levels of Notch activity was explored by monitoring Notch reporter activity after ligand overexpression. We used two gene constructs in which DsRed or luciferase reporter genes were driven by multimeric CSL binding site repeats (12×CSL-DsRed or 8×CSL-Luc) (Jeffries et al., 2002; Hansson et al., 2006). These constructs responded to different levels of Notch activity *in vitro* (supplementary material Fig. S3A). They were active in the otic vesicle (supplementary material Fig. S3B-D), induced by NICD transfection (supplementary material Fig. S3C) and repressed by Notch blockade (supplementary material Fig. S3D). The results of cotransfection of the 12×CSL-DsRed or 8×CSL-Luc reporters with Dl1 or Jag1 are shown in Fig. 4A,B. DsRed reporter activity was measured by direct red fluorescence or by quantifying DsRed mRNA levels (Fig. 4A). Luciferase reporter activity was measured by a colorimetric enzymatic assay on protein extracts from otic vesicles (Fig. 4B). In all cases, levels of reporter activity were higher after Dl1 overexpression than after Jag1 by 2- to 6-fold,

Development (2014) 141, 2313-2324 doi:10.1242/dev.108100

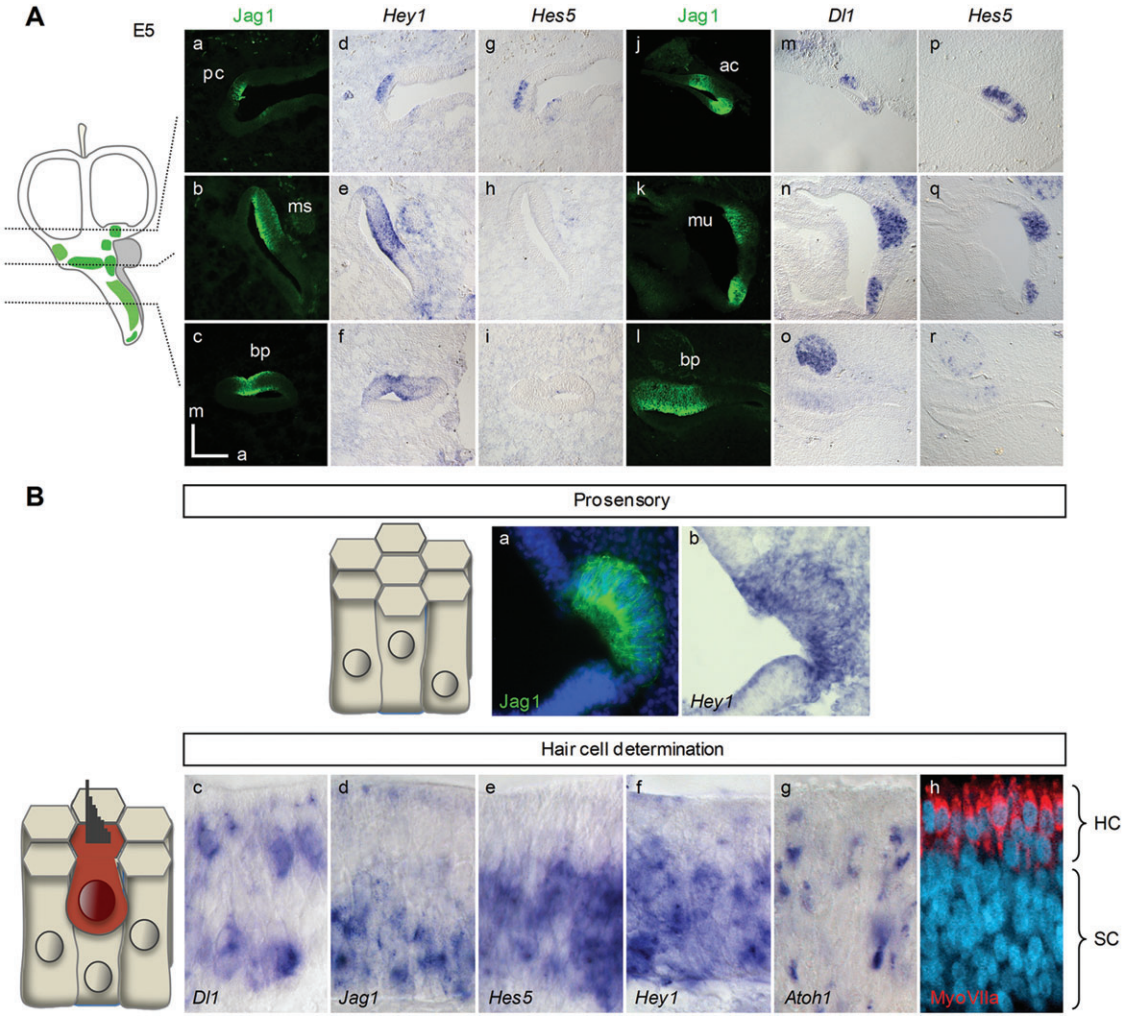

Fig. 1. Jag1 and Dl1 are associated with different Notch targets. (A) Alternate serial coronal sections of chick E5 otocyst processed for IHC against Jag1 (a-c,j-l) and ISH for *Hey1* (d-f), *Hes5* (g-i,p-r) and *Dl1* (m-o). The diagram on the left indicates the level of the section. Orientation: m, medial; a, anterior. (Ba,b) Prosensory patch immunostained for Jag1 (a) and processed for ISH for *Hey1* (b). (Bc-h) Sensory patches probed for *Dl1* (c), *Jag1* (d), *Hes5* (e), *Hey1* (f), *Atoh1* (g) and immunostained for MyoVIIa (h). The diagram represents the arrangement of the cells in the prosensory and sensory (red) patches. ac, anterior crista; pc, posterior crista; ms, macula sacularis; mu, macula utricularis; bp, basilar papilla; HC, hair cells; SC, supporting cells.

suggesting that the strength of the Notch signal induced by Jag1 is much lower than that induced by Dl1.

A key question in understanding the combined function of Jag1 and Dl1 in the sensory patches is to resolve which signal is evoked when both ligands are expressed together. To address this we modeled phenomenologically the signal induced by each ligand. We considered that each ligand drives the same type of signal but with different strengths (Fig. 2, Fig. 3, Fig. 4A,B), and that both ligands use common resources, such as the Notch1 receptor (Adam et al., 1998; Abelló et al., 2007) (Eqn 1). According to the model, when resources become limiting, competition between Dl1 and Jag1 results in an overall signal that is lower than the signal driven by Dl1 in the absence of Jag1 (Fig. 4C). This happens because Jag1 is a weak signaling ligand compared with Dl1 ($\epsilon<1$, with ϵ being the ratio of Jag1-driven over Dl1-driven Notch saturated signal). In this case, Jag1 becomes an inhibitor of Notch signaling despite it driving signaling (Fig. 4C). This was experimentally confirmed by the co-expression of Jag1 and Dl1 together with Notch reporter constructs (Fig. 4A,B). Jag1 reduced the signal evoked by Dl1, suggesting that Jag1 and Dl1 compete for the activation of Notch. The combined Jag1 plus Dl1 signal was closer to that of Jag1 than to that of Dl1 (Fig. 4A,B), indicating that Jag1 has a higher apparent affinity than Dl1 for Notch (Fig. 4C,D).

Differences in the signaling strength of Jag1 and Dl1 enable hair cell patterning when both ligands are present

Knowing that Jag1 drives a weaker signal than Dl1 and that it competes for signaling, we examined whether this is relevant for the transition from prosensory to sensory states. We developed a combined model for lateral induction and lateral inhibition driven by Jag1 and Dl1, respectively. As with lateral inhibition, lateral induction relies on Notch signaling but through opposite regulation of the ligand (supplementary material Fig. S4). This was confirmed by the inhibitory effect of the Notch blocker LY411575 on the induction of *Jag1* by Jag1 (Fig. 5A and Fig. 3A). The model presented here is based on Notch signaling by Jag1 and Dl1 (Eqn 1), together with the circuits that regulate ligand expression (Eqns 2-4, Fig. 5B, Materials and Methods). We also introduced Atoh1 as the proneural gene that drives the initiation of Dl1 expression, the repression of Atoh1 by Notch (Takebayashi et al., 2007; Doetzlhofer et al., 2009) (Eqn 4), and its autoactivation (Helms et al., 2000). Hey1 and Hes5 were not included in the model for

Development (2014) 141, 2313-2324 doi:10.1242/dev.108100

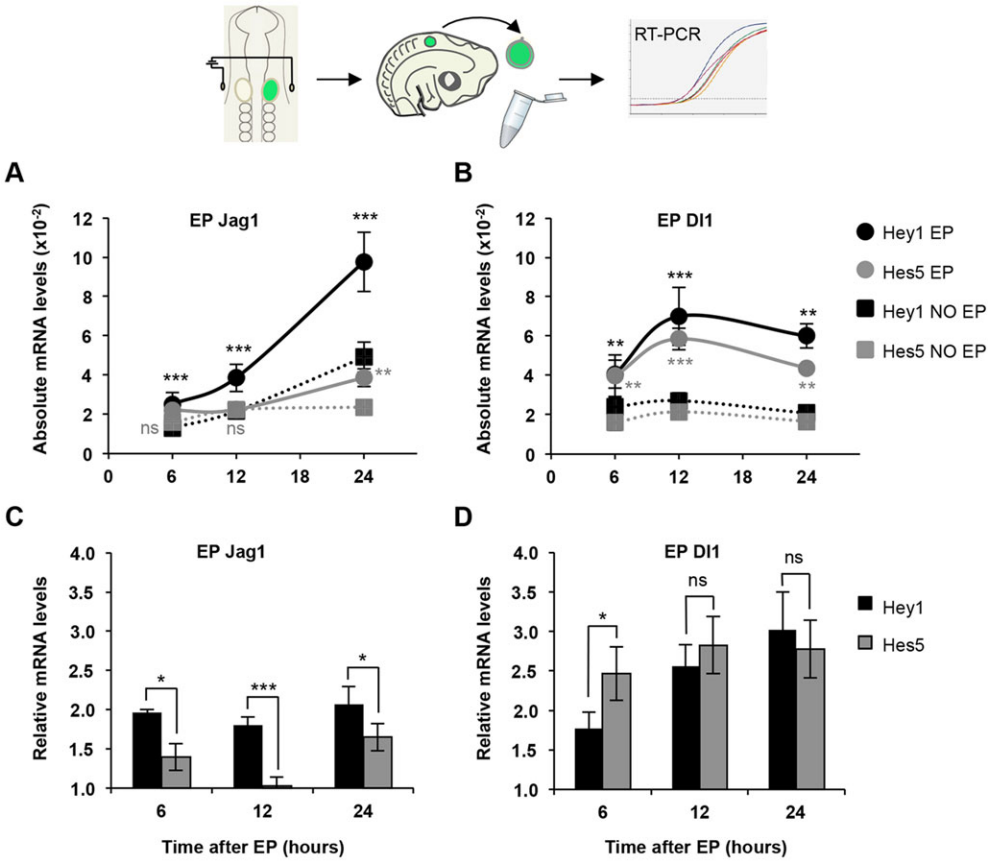

Fig. 2. Jag1 and Dl1 differentially regulate *Hey1* and *Hes5*. Timecourse of absolute mRNA levels ($2^{-\Delta Ct}\times10^{-2}$) of *Hey1* and *Hes5* after electroporation (EP) with hJag1 (A) or cDl1 (B). Relative mRNA levels ($2^{-\Delta\Delta Ct}$) of *Hey1* and *Hes5* after electroporation with hJag1 (C) or cDl1 (D). The diagram at the top illustrates the experimental procedure. Values in C and D are relative to unelectroporated otic vesicles (EP-hJag1: 6 h, *n*=4; 12 h, *n*=5; 24 h, *n*=7; EP-cDl1: 6 h, *n*=5; 12 h, *n*=5; 24 h, *n*=4). Statistical significance of *Hey1* and *Hes5* ($2^{-\Delta Ct}$) was tested by comparing individual ΔCt values (A,B) or fold induction (C,D) from experimental and unelectroporated samples. For all bar chart data shown: error bars indicate s.e.m.; ***P<0.001; **P<0.01; *P<0.05; ns, non significant (Student's *t*-test).

simplicity; they behaved similarly with respect to the regulation of ligands (not shown) and can be taken as simple readouts of the signal level.

First, we tested the model for Jag1 as the only ligand, a situation that occurs in the prosensory state. In this case, Jag1 drives bistability of homogeneous coherent states (Fig. 5C, green area of lateral induction), enabling Jag1 propagation (Fig. 5D; supplementary material Movie 1), in agreement with the work of Matsuda et al. (2012). This mimics the results of the gain of function of Jag1 (Hartman et al., 2010; Pan et al., 2010; Neves et al., 2011) (Fig. 5A). The bistable regime of lateral induction (i.e. the range of Jag1 production) enlarges with the strength of Jag1-driven signaling, and requires a minimal signaling strength (Fig. 5C).

The transition from the prosensory to the hair cell specification stages was simulated by the expression of Dl1 in a background of Jag1. For a weak Jag1-driven signal ($\epsilon<1$), an appropriate fine-grained patterning of lateral inhibition emerged from a Jag1 homogeneous state upon activation of Atoh1 expression (Fig. 5E, blue area). This pattern was formed by cells expressing Atoh1 and Dl1 (hair cells), which were surrounded by cells expressing Jag1 (supporting cells, Fig. 5F). Atoh1 autoactivation conferred robustness to its maintenance (supplementary material Fig. S5). The model, therefore, reproduced correctly the hair cell determination state. In addition, it revealed that the differential signaling strength between Jag1 and Dl1 was crucial for the transition from the prosensory to the sensory states. Equal signaling strength for both ligands ($\epsilon=1$) enabled hair cell patterning only if Jag1 expression was reduced so as to forbid the emergence of supporting cells expressing Jag1 (Fig. 5G, left). By contrast, a weak Jag1 signaling strength facilitated hair cell patterning (Fig. 5G, middle and right). This is because Jag1, as a weak signal inducer, behaves as a partial agonist of Notch, i.e. Jag1 inhibits Notch signaling in the presence of Dl1 (Fig. 4). Under these circumstances, adjacent cells expressing both Jag1 and D1 mutually inhibit each other, even for low Dl1 levels (supplementary material Fig. S6 and Movie 2). This behavior is in contrast to the mutual activation that Jag1 drives between adjacent cells when expressed alone (supplementary material Fig. S6).

These results indicate that weak Jag1 signaling ($0<\epsilon<1$) may drive the prosensory state (Fig. 5C) and also facilitates hair cell patterning (Fig. 5G). Only a band of weak Jag1 signaling strengths enables the transition between these two states as triggered by Atoh1 (Fig. 5E).

The signature of Jag1 in facilitating hair cell patterning is a bias in cell fate commitment

The model predicts that Jag1 facilitates lateral inhibition by competing with Dl1 signaling. To test this, we analyzed the effects of manipulating Jag1 levels at the onset of hair cell determination. hJag1 or Jag1 siRNA were expressed in E3.5 chicken otocysts and the sensory domains examined 3 days after electroporation (Fig. 6). In none of these conditions was hair cell patterning substantially altered (Fig. 6A, whole-mount preparations in the top row). The general organization of the patch and the density of hair cells were similar in all conditions (compare control and Jag1 EP in Fig. 6A, bottom row, and 6B). The loss of function of Jag1 reduced Sox2 expression (supplementary material Fig. S7) and slightly decreased the density of hair cells (Fig. 6B). These results suggest, contrary to expectations, that Jag1 is not involved in hair cell patterning.

To clarify this point, we evaluated model predictions further by mimicking gain- and loss-of-function experiments with numerical

Development (2014) 141, 2313-2324 doi:10.1242/dev.108100

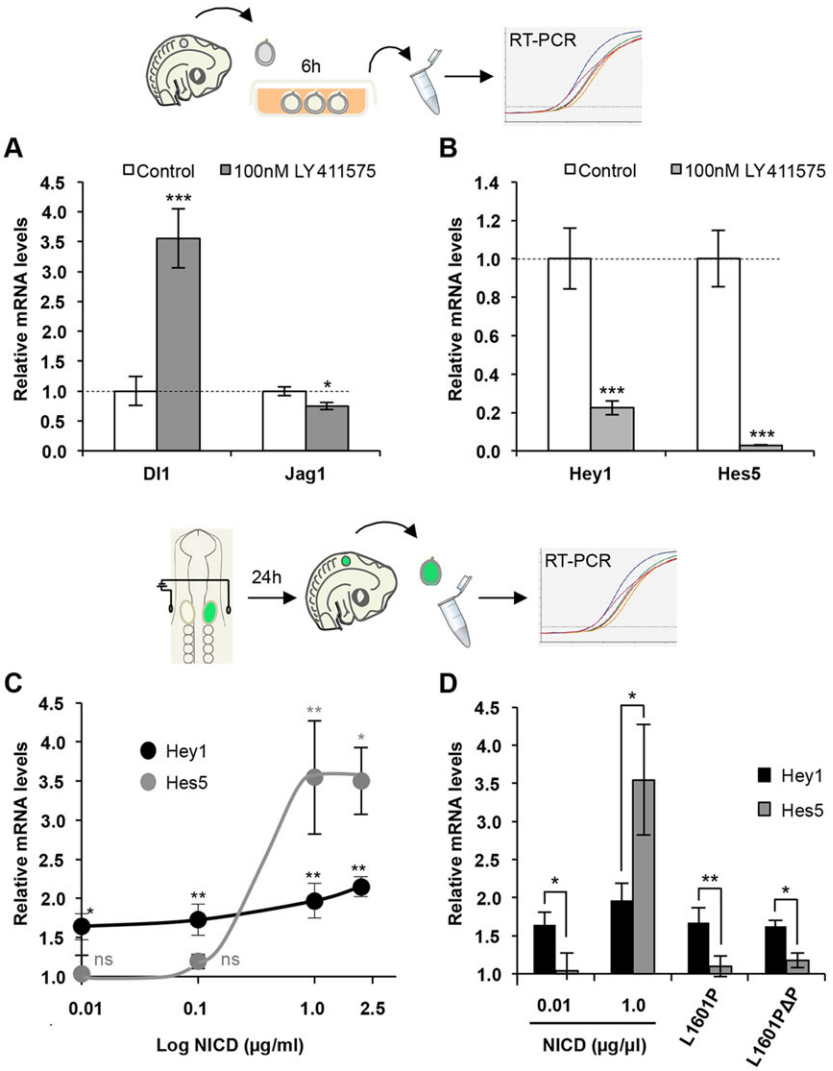

Fig. 3. Levels of Notch activity determine target selection. Relative mRNA levels of *Dl1* and *Jag1* (A) and *Hey1* and *Hes5* (B) at E3 after Notch inhibition for 6 h with 100 nM LY411575. (C) Semi-log plot of relative mRNA levels of *Hey1* and *Hes5* in E2 otic vesicles after 24 h electroporation with increasing concentrations of NICD. (D) Relative mRNA levels of *Hey1* and *Hes5* after electroporation with 0.01 µg/µl NICD and with 1 µg/µl NICD, L1601P or L1601PΔP. Values are relative to unelectroporated otic vesicles (A,B, *n*=9; C, *n*=4-5; D, *n*=3-5).

simulations (Materials and Methods). As *in vivo*, hair cell patterning persisted in both cases (Fig. 6C; see supplementary material Fig. S8 for an exploration of the range of validity of the model). When the same simulations were performed in the absence of Atoh1 autoactivation, however, hair cell patterning was totally disrupted (supplementary material Fig. S9). This indicates that Atoh1 autoactivation buffers the role of Jag1 by providing robustness to the patterning process.

If patterning is so robust, is there a signature for Jag1 as a facilitator of hair cell patterning? Numerical simulations revealed a consistent trend: adjacent Jag1-electroporated cells and non-electroporated cells tended to become supporting and hair cells, respectively (Fig. 6C). This resulted in a tendency of Jag1-positive cells to avoid the hair cell fate and become supporting cells, which was particularly evident at low electroporation densities, where the probability of contacts between electroporated and non-electroporated cells was high (Fig. 6C). We reasoned that this behavior resulted from the reduction of Notch signaling elicited by Jag1 when competing with Dl1. Cells carrying Jag1 reduced the Notch signal in neighboring non-electroporated cells and released the Notch-mediated Atoh1 inhibition, thereby promoting the hair cell fate choice. This, in turn, favored Jag1-delivering cells to become supporting cells. The opposite trend, although weaker, was found for numerical simulations of loss of function (Fig. 6C; supplementary material Fig. S8). In summary, modeling suggests that weak Notch signaling driven by Jag1 results in a specific bias in hair cell and supporting cell determination, which becomes the signature feature of Jag1 in facilitating hair cell patterning.

We then asked whether this signature is measurable *in vivo* by a more detailed analysis of the Jag1 gain- and loss-of-function experiments in the chick embryo (Fig. 6D). The experiments show that cells carrying the hJag1 transgene were less likely to differentiate as hair cells, as predicted by the model. The proportion of hair cells carrying hJag1 was always smaller than the total fraction of electroporated cells (Fig. 6D). As in the numerical simulations, this was more evident at moderate electroporation densities (Fig. 6D, low EP). Also in agreement with the model, loss-of-function experiments showed a weak opposite trend (Fig. 6D). Therefore, the signature of Jag1 as a facilitator of hair cell patterning was evident *in vivo* as a cell fate bias.

DISCUSSION

Dl1 and Jag1 signal differently in the inner ear

The results show that Dl1 and Jag1 drive Notch signaling at different strengths, eliciting differential expression of Hey1 and Hes5. The expression of Hes5 and Hey1/2/L and their sensitivity to gamma-secretase inhibitors has also been reported in the mouse (Hayashi et al., 2008; Doetzlhofer et al., 2009). Interestingly, Hes5 is more sensitive than Hey1 to treatment with DAPT, suggesting that it requires higher levels of intracellular Notch activity (Doetzlhofer

Development (2014) 141, 2313-2324 doi:10.1242/dev.108100

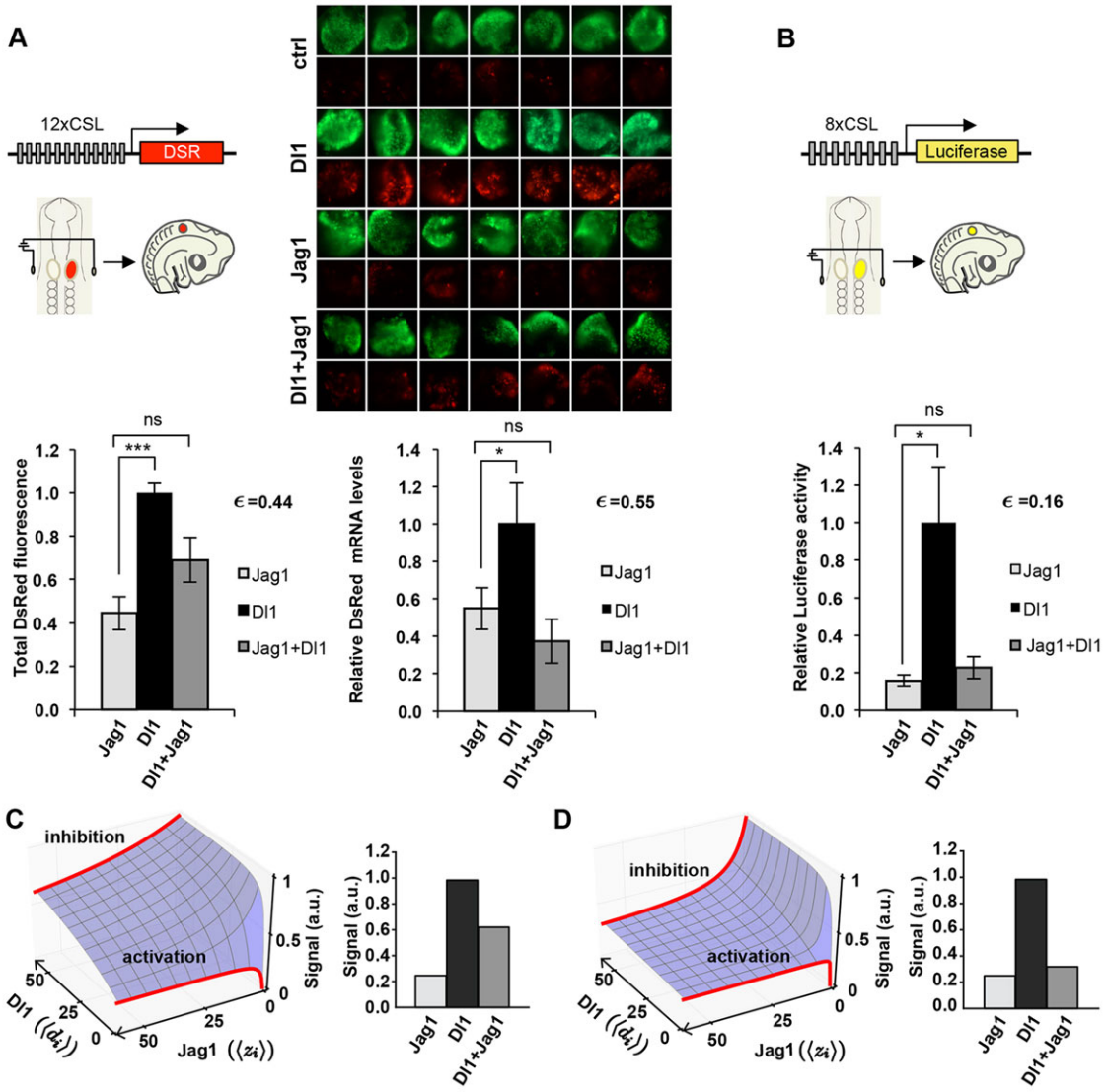

Fig. 4. Different Notch ligands induce different Notch signaling strength. (A) Otic vesicles co-electroporated with the 12xCSL-DsRed (DSR) reporter construct and GFP (control), Dl1/GFP, Jag1/GFP or Jag1/GFP+Dl1/GFP. Ligands were used at 1 μg/μl, and total DNA was adjusted with GFP to be constant in all conditions. GFP was used to monitor the electroporation. Photomicrographs were used for quantification of red fluorescence and the results are plotted in the bar chart (below left; n=23, n=27 and n=7 from three different experiments). The bar chart (below right) shows quantification of relative DsRed mRNA levels as assessed by qRT-PCR (n=3-4). (B) Otic vesicles co-electroporated with the 8xCSL-Luc reporter and Dl1/GFP, Jag1/GFP or Jag1/GFP+Dl1/GFP. Beneath is shown the relative levels of normalized luciferase activity in the different experimental conditions (n=3-10). (C) Stationary signal (s_i value when Eqn 1 is set to zero) as a function of the ligand concentrations for Jag1:Dl1 saturated signal of 1:4 (ϵ=0.25), but with the same apparent affinity for Notch (ϵ_r=1). The bar chart shows the stationary signal for $\langle d_i \rangle$=0 and $\langle z_i \rangle$=60 (Jag1), $\langle d_i \rangle$=60 and $\langle z_i \rangle$=0 (Dl1), and $\langle d_i \rangle$=$\langle z_i \rangle$=60 (Dl1+Jag1). Competition between ligands changes the role of Jag1 (red lines) when Dl1 is present, driving signal reduction (inhibition), in qualitative agreement with the experimental data (A,B). a.u., arbitrary units. (D) As C, but when the apparent affinity of Jag1 for Notch is higher than that of Dl1 (ϵ_r=10).

et al., 2009). Moreover, Hayashi et al. (2008) showed that the concentration of DAPT required to inhibit Notch signaling during lateral inhibition is lower than for the prosensory phase, suggesting that Hes5 and lateral inhibition share a similar sensitivity to Notch.

Alternative cellular behaviors dependent on Notch levels have been reported in relation to the decision between cell proliferative and cell arrest states (Mazzone et al., 2010; Perdigoto et al., 2011; Ninov et al., 2012). In the prosensory patches, sensory progenitors proliferate (Murata et al., 2009), whereas in the differentiating sensory organs the hair cells exit the cell cycle and differentiate (Chen and Segil, 1999) while supporting cells enter a quiescent state (Oesterle and Rubel, 1993). One possibility is that gene regulation and cellular function depend on the different levels of Notch signaling elicited by the different ligands. Recently, Liu et al. (2013) showed that Notch activity is almost undetectable during prosensory stages, but increases during hair cell determination. This fits well with our results and with the notion that the prosensory state is driven by Jag1 and that hair cell patterning involves strong Dl1 signaling.

Notch ligands: lateral induction and lateral inhibition

In the inner ear, expression patterns and functional studies suggest that lateral induction and inhibition are associated with different Notch ligands that initiate signaling, with Jag1 driving lateral induction and Dl1 lateral inhibition (Brooker et al., 2006; our present results). The association of Dl1 with lateral inhibition is a general theme in neural development (Henrique et al., 1995; Adam et al., 1998; Kageyama et al., 2010) and that of Jag1 with lateral induction

Development (2014) 141, 2313-2324 doi:10.1242/dev.108100

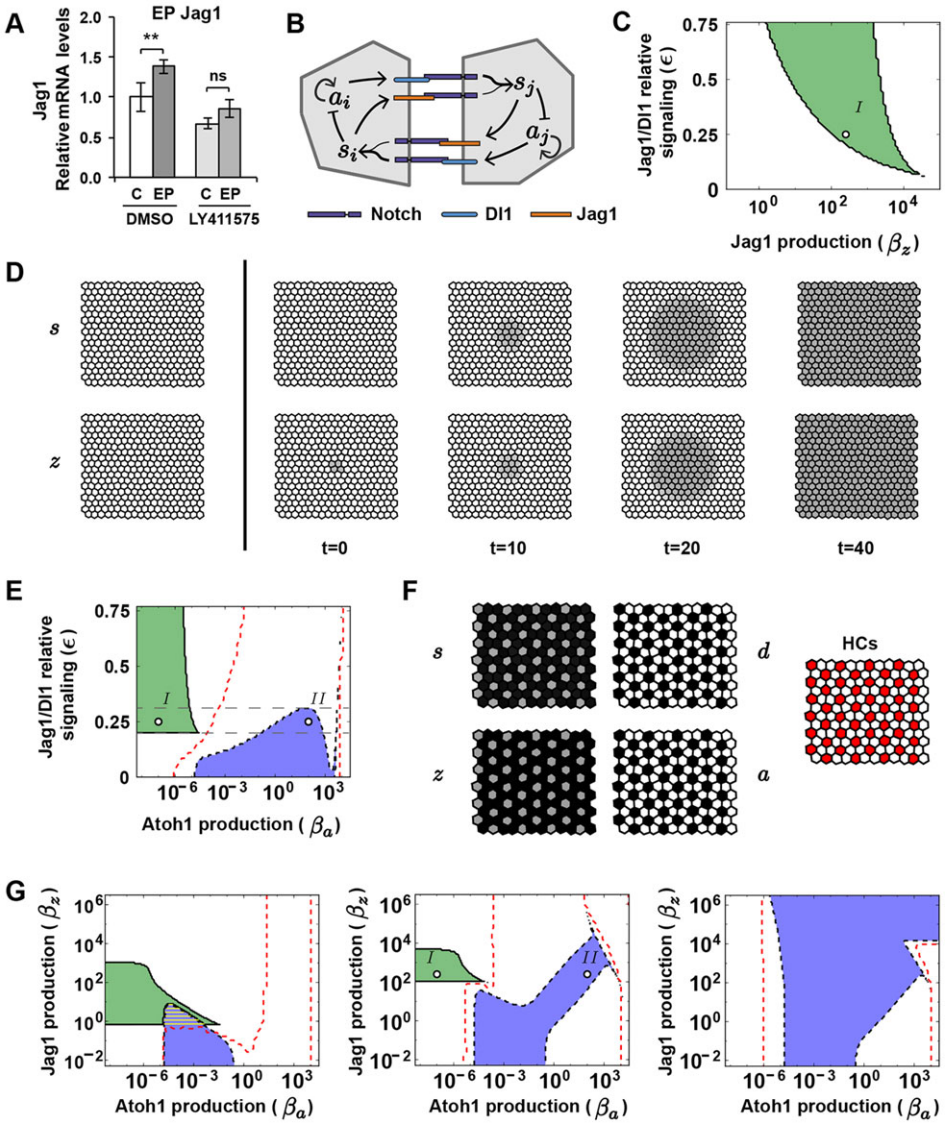

Fig. 5. Weak Jag1 signaling strength enables the transition from lateral induction to lateral inhibition. (A) Jag1 induction is Notch dependent. E2 otic vesicles were electroporated with hJag1, allowed to develop for 4 h *in ovo* and then cultured *in vitro* for 12 h. mRNA levels of cJag1 are shown from electroporated (EP) and unelectroporated (C) otic vesicles incubated in DMEM, with or without 100 nM LY411575. Values are relative to unelectroporated otic vesicles (n=5). (B) Schematic of the model (a_i, s_i: Atoh1 and Notch activities in cell i). Arrows denote activation, blunt arrows indicate inhibition. (C) Parameter region [green, computed through LSA (see Materials and Methods)] where mutual activation between Jag1 and the Notch signal induces bistability of homogeneous states in the absence of Dl1 ($\beta_a=10^{-7}$). Bistability requires a minimal Jag1 signaling strength (ϵ). The white region corresponds to one single homogeneous stable state. (D) Bistability enables Jag1 (z) and signal (s) propagation over time from a stable tissue state with low levels of Jag1 and of the signal (left) to a homogeneous stable state with higher levels of Jag1 and of the signal (right, t=40 panel), after Jag1 is locally introduced at time t=0 (in four central cells, with Jag1 amplitude 1). Levels of ligand and signal are in grayscale from white (low) to black (high). Parameter values are of point I in C,E. (E) Bistable (green) and fine-grained pattern formation (blue) regions computed through LSA in the parameter space of Jag1 signaling strength relative to that of Dl1 (ϵ) and of Atoh1 production (β_a) for β_z=250. The area within the red lines is the region in which the fine-grained pattern for β_a=100 and ϵ=0.25 is maintained (see Materials and Methods). (F) Stable fine-grained pattern at point II in E with color codes as in D and hair cells in red (d stands for Dl1). (G) Regions as in E for the parameter space of Jag1 and Atoh1 productions for ϵ=1 (left), ϵ=0.25 (middle) and ϵ=0 (right). The pattern is not stationary in the hatched region of G (left). Patterns evaluated for maintenance correspond to $\beta_a=\beta_z$=0.01 (left) and β_a=100, β_z=250 (middle, right) for the corresponding ϵ values. Additional parameter values are detailed in Materials and Methods.

has been shown also in the lens (Le et al., 2009), developing pancreas (Golson et al., 2009), early hematopoiesis (Robert-Moreno et al., 2008) and angiogenesis (Benedito et al., 2009). However, this correspondence does not seem to hold for all situations; for example, Jag1 selects V1 neuroblasts in the neural tube by lateral inhibition (Ramos et al., 2010). In the inner ear, Jag1 and Dl1 are oppositely regulated by Notch signaling, which readily accounts for their association into the circuits of lateral induction and of lateral inhibition, respectively. The inhibition of Dl1 by Notch has been associated with the repressor effect of Hes/Hey genes on bHLH proneural genes (Kageyama et al., 2010), but the activation of Jag1 by Notch remains poorly understood (Katoh, 2006).

Modeling predicts that the function of Jag1 alone is distinct from that in the presence of Dl1 because of competition for common resources and their different signaling strengths. Therefore, it is likely that context determines the behavior of Dl1 and Jag1 ligands in different tissues. The interaction of different ligands with the Notch receptor is modulated by various factors, such as Fringe

Development (2014) 141, 2313-2324 doi:10.1242/dev.108100

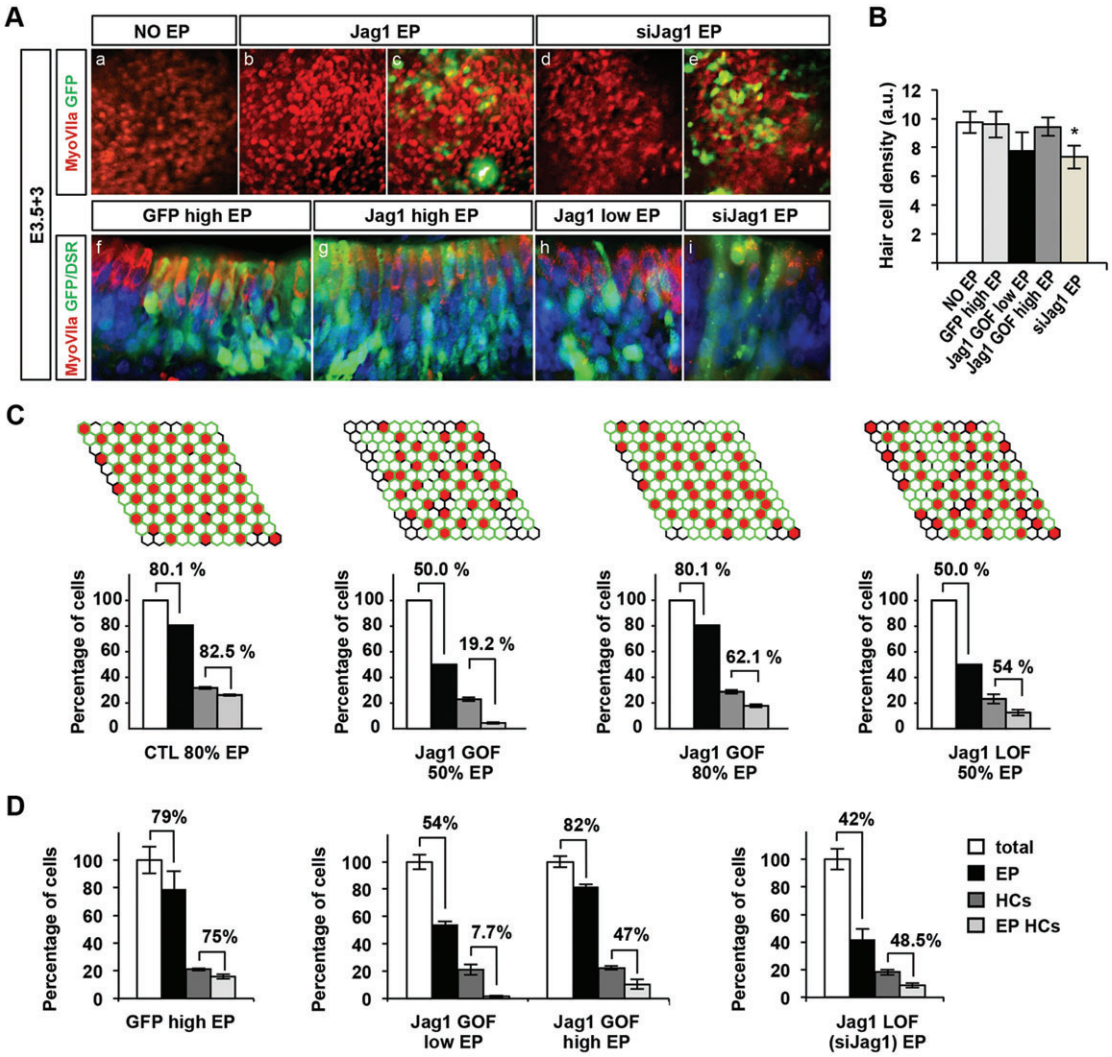

Fig. 6. Hair cell patterning is robust, yet Jag1 biases cell fate. (A) Whole-mount preparations of sensory organs stained for MyoVIIa (a-e) and GFP (c,e). Otocysts were electroporated (EP) with GFP/DsRed, hJag1 and Jag1 siRNA (siJag1) at E3.5 and analyzed after 3 days. Cross-sections of sensory patches stained for MyoVIIa, GFP/DsRed and with DAPI after GFP (f), high and low hJag1 (g,h) and siJag1 (i; original colors inverted for clarity) electroporations. (B) Hair cell density in the conditions indicated. (C) Snapshots (top) and quantitative results (bottom) for numerical simulations of Jag1 gain of function (GOF) and loss of function (LOF). Data correspond to the stationary state. Hair cells are in red; cells outlined in green represent electroporated cells (percentage of electroporated cells indicated). Bar charts show mean±s.e.m., with color code as in D. Simulations were performed for β_a=100, β_z=250 and ϵ=0.25 (point II in Fig. 5E,G) on the homogeneous stationary state of low Jag1. Tests with initial conditions at the high Jag1 stationary state of point I gave similar results (not shown). CTL, control electroporations. (D) Number of electroporated cells (as percentage of the total) after the electroporation of GFP (left), low (54%) or high (82%) Jag1 (middle), and siJag1 (right). Values are mean±s.e.m. of n=4-8 samples from at least three independent experiments. Values indicate the percentage of electroporated cells and the percentage of electroporated hair cells. A,B,D, experimental data; C, numerical simulation results.

glycosylation that potentiates Dl1-induced Notch signaling while hampering Jag1 (Bruckner et al., 2000; Haines and Irvine, 2003; Benedito et al., 2009). Lunatic fringe is expressed in sensory regions of the inner ear (Morsli et al., 1998; Cole et al., 2000) and is a likely candidate to maintain low-level Jag1-driven signaling in sensory domains.

Levels of Notch signaling and competition: a novel interaction between Dl1 and Jag1

The model presented in this paper suggests that Notch levels play a key role in resolving the confrontation between Jag1 and Dl1 in otic sensory progenitors. But, in addition, the model yields a non-trivial behavior according to which Jag1 actually facilitates lateral inhibition patterning. The specific role of Jag1 results from the competition between Dl1 and Jag1 for Notch signaling through the Notch receptor. When Jag1 signals less than Dl1, Jag1 may act as a dominant-negative or a partial agonist of the Notch receptor (Buchler et al., 2003), reducing overall Notch signaling. This situation resembles that found in cis-inhibition of Notch signaling, in which Dl1 ligand in a cell competes with Dl1 ligand in neighboring cells to bind to Notch receptor (Formosa-Jordan and Ibañes, 2014). In the context of inner ear development, cis-inhibition does not occur (Chrysostomou et al., 2012), but the competition between Dl1 and Jag1 ligands results in a similar effect on the signal. Our results indicate that, upon Atoh1 expression, Jag1 switches from increasing overall signaling and driving lateral induction to effectively decreasing Notch signaling and facilitating hair cell patterning. This facilitation arises from the mutual inhibition between adjacent equivalent cells driven by Jag1 when competing with Dl1 (supplementary material Fig. S6).

Development (2014) 141, 2313-2324 doi:10.1242/dev.108100

Given the robustness of hair cell patterning, the signature of Jag1 is a bias in the cell fate rather than a large disturbance of the pattern. We did not observe the effects described in mouse cochlear explants by Zine et al. (2000), who showed an excess of outer hair cells after a 5-day treatment with antisense oligos targeted against *Jag1*. Our work focuses instead on chick vestibular maculae, in which, in our hands, Jag1 loss results in the loss of supporting cell identity, although this does not seem sufficient to switch to the hair cell fate. The potential effects of newly added cells during patterning and of other morphogenetic mechanisms remain to be elucidated.

The results suggest that the robustness of hair cell patterning to changes in Jag1 expression arises mainly from the autoactivation of Atoh1. Although Atoh1 autoactivation neither facilitates nor promotes pattern initiation, Atoh1 autoactivation maintains patterning once it is established and stabilizes the final pattern. This is in agreement with recent results showing that once sensory progenitors start to highly express Atoh1 and subsequently Dl1, they cannot be prevented from becoming hair cells (Driver et al., 2013). This might also underlie the observation by Chrysostomou et al. (2012) of the generation of hair cells in direct contact with several neighboring cells expressing high levels of Dl1.

In summary, the combination of opposed feedback regulatory mechanisms, differential signaling strength and competition between Jag1 and Dl1 for Notch is crucial for orchestrating lateral induction and lateral inhibition during ear development. Through the positive loop of Jag1, Notch establishes a coherent domain of low Notch activity, in which Notch signaling is expanded by lateral induction. Notch, in turn, induces Sox2 expression and bHLH targets that prevent differentiation. The result is the specification of the prosensory patches. Upon Atoh1 expression, both Dl1 and Jag1 mediate the inhibition of neighbors, generating the hair cell/supporting cell lattice, and patterning follows the rules of lateral inhibition. In other words, Jag1 exhibits a new function in facilitating lateral inhibition and hair cell patterning; this is because, in the presence of Dl1, both ligands compete for the same resources. Since Jag1 is a weaker activator, it acts as a partial agonist of Notch receptor and effectively inhibits signaling. If both Dl1 and Jag1 were to signal with the same strength, lateral induction and lateral inhibition would conflict and the pattern would be disrupted. Instead, weak Jag1 signaling enables Jag1 to drive prosensory patches when acting alone, but then to switch its role upon Dl1 expression.

MATERIALS AND METHODS

In ovo electroporation

A DNA mix containing the desired vector(s) mixed with Fast Green was injected onto the otic cup of HH12-14 chick embryos (Neves et al., 2011) or into HH20-21 otic vesicles (Kamaid et al., 2010). Jag1 overexpression in 3-day experiments was confirmed by immunohistochemistry. Animal procedures were approved by the Ethical Committee of the Parc de Recerca Biomèdica de Barcelona.

Loss-of-function experiments

Stealth cJag1 RNAi or scrambled Stealth controls (Life Technologies; supplementary material Table S1) were mixed with GFP or DsRed and Fast Green and injected at 30 µM into HH20-21 otic vesicles. The effects were assessed 1-3 days after electroporation (Fig. 6). Efficiency of Jag1 silencing was assessed by immunostaining (supplementary material Fig. S7). Stealth RNAi is stabilized against nuclease degradation and stable for at least 3 days in culture (Life Technologies).

In vitro culture of otic vesicles

Otic vesicles were dissected from HH20 chick embryos, grown in culture (Pujades et al., 2006) and incubated with either DMEM or 100 nM LY411575 (Dr Kim Dale, University of Dundee, UK) for 6 h (Fig. 3A,B). In some experiments, HH12-14 otic cups were electroporated with hJag1 and allowed to develop for 4 h *in ovo*. Electroporated and control otic vesicles were then dissected and further cultured with DMEM or media supplemented with 100 nM LY411575 for 12 h (Fig. 5A).

In situ hybridization (ISH) and immunohistochemistry (IHC)

Embryos were processed for ISH and IHC as described (Acloque et al., 2008; Neves et al., 2007). Primary antibodies were: anti-Jag1 rabbit polyclonal (Santa Cruz Biotechnology, sc-8303, H-114, 1:50), anti-GFP rabbit polyclonal (Clontech, 632460, 1:400), anti-MyoVIIa mouse monoclonal (Developmental Studies Hybridoma Bank, 138-1, 1:100), anti-Sox2 goat polyclonal (Santa Cruz, Y-17, 1:400) and anti-DsRed rabbit polyclonal (Takara, 632496, 1:400). Secondary antibodies were Alexa Fluor 488-, 568- and 594-conjugated anti-mouse, anti-goat and anti-rabbit (Molecular Probes Invitrogen, 1:400). Sections were counterstained with DAPI (100 ng/ml, Molecular Probes) and mounted in Mowiol (Calbiochem). Fluorescence was analyzed by conventional fluorescence microscopy using a Leica DMRB with Leica CCD camera DC300F and images were processed with Adobe Photoshop. Some otic vesicles were photographed and analyzed without sectioning. Fluorescence of each otic vesicle was measured and corrected for the area electroporated using ImageJ (Fig. 4A): corrected total fluorescence (CTF)=integrated density−(electroporated area×mean background fluorescence).

Quantitative real-time PCR (qRT-PCR)

RNA was isolated using the RNeasy Micro or Mini Kit (Qiagen) including a step of in-column digestion with DNase. cDNA was synthetized from 15 ng RNA with Superscript III DNA polymerase (Invitrogen) and random primers (Invitrogen), and reverse transcribed in duplicate. qRT-PCR was carried out using 1 µl cDNA, SYBR Green Master Mix (Roche) and gene-specific primers (Invitrogen; supplementary material Table S2) in a LightCycler480 (Roche). Each transcribed in duplicate cDNA was used as template for each pair of primers in triplicate PCR reactions.

β-Gal and luciferase enzymatic assays

Protein extracts were prepared using Reporter Lysis Buffer (Promega; 10 µl per otic vesicle). β-Gal activity and luciferase activity were determined as previously described (Neves et al., 2012). Luciferase activity was normalized for the level of transfection using the β-Gal enzymatic reaction.

Statistics

Results are shown as mean±s.e.m. of n experiments as indicated in figure legends. Statistical significance was assessed using Student's t-test.

Mathematical model

We propose a model for two ligands, Dl1 (d) and Jag1 (z), that activate the Notch signal (s) in neighboring cells, which in turn regulates the ligands. It is based on the one-ligand model of Collier et al. (1996) with graded activation of the signal (Sprinzak et al., 2010). The model couples the single-ligand circuits of lateral induction (for Jag1) and of lateral inhibition (for Dl1) through the Notch signal. Previous models explored lateral induction (e.g. Owen et al., 2000; Savill and Sherratt, 2003; Webb and Owen, 2004; Matsuda et al., 2012) but none combined it with a lateral inhibition circuit. The non-dimensional dynamics in any i cell, with Atoh1 being described by variable a, read:

$$\frac{ds_i}{dt} = \frac{\epsilon\epsilon_r\langle z_i\rangle + \langle d_i\rangle}{1+\epsilon_r\langle z_i\rangle + \langle d_i\rangle} - s_i, \quad (1)$$

$$\frac{dz_i}{dt} = \nu_z\left\{\frac{\beta_z s_i^{h_z}}{\theta_z^{h_z} + s_i^{h_z}} - z_i\right\}, \quad (2)$$

$$\frac{dd_i}{dt} = \nu_d\left\{\frac{\beta_d a_i^{h_d}}{1 + a_i^{h_d}} - d_i\right\}, \quad (3)$$

$$\frac{da_i}{dt} = \nu_a\left\{\frac{\beta_a}{1 + b_a s_i^{h_{a1}}}\left(1 + \frac{\alpha a_i^{h_{a2}}}{\theta_a^{h_{a2}} + a_i^{h_{a2}}}\right) - a_i\right\}, \quad (4)$$

Development (2014) 141, 2313-2324 doi:10.1242/dev.108100

where $\langle z_i \rangle$ and $\langle d_i \rangle$ stand for the corresponding ligand concentration averaged over neighboring cells to cell i in a two-dimensional lattice of irregular cells (Podgorski et al., 2007). ϵ is the ratio between the maximal signal induction driven by Jag1 and that by Dl1. ϵ_r is the ratio between Jag1- and Dl1-mediated apparent affinities to Notch. Competition between Jag1 and Dl1 for common resources of Notch signaling is included in the denominator of Eqn 1. $\nu_{z,d,a}$ set the time-scales of Jag1, Dl1 and Atoh1 with respect to Notch signal. $\beta_{z,d}$ stand for the production of Jag1 and Dl1. β_a sets the basal activation of Atoh1 and $\alpha\beta_a$ its autoactivation. $h_{d,z,a1,a2}$ are cooperativities to model the nonlinearities of the processes, θ_z and $b_a^{-h_{a1}}$ are the threshold value of Notch signal at which Jag1 is activated and Atoh1 is repressed, respectively, at half its maximal value. θ_a is the Atoh1 threshold value for Atoh1 autoactivation. Parameter values are $\nu_z=\nu_d=\nu_a=1$, $h_{a1}=h_{a2}=h_z=4$, $h_d=1$, $\beta_d=10^4$, $\alpha=10^8$, $\theta_z=0.8$, $b_a=5\times10^4$, $b_a=5\times10^4$ and $\epsilon_r=10$ unless otherwise stated in figure axes and captions.

Mathematical analysis

Stationary homogeneous states of Eqns 1-4 ($\frac{dx_i}{dt}=0 \forall i$ and $x_i=x_j\ \forall i,j$, where x stands for each variable) were searched with a custom-made program for root-finding through the bisection method. Stability of these solutions in a perfect hexagonal array of cells to small perturbations was mathematically evaluated through a linear stability analysis (LSA) as in Formosa-Jordan and Ibañes (2009). It yielded the Routh-Hurwitz conditions (Murray, 2002) detailed in supplementary material Fig. S5. This analysis explored the parameter space to find the parameter regions that can sustain lateral induction with ligand propagation (i.e. bistable regions with two stable homogeneous states; green in Fig. 5C,E,G) and those where the fine-grained pattern of lateral inhibition can emerge from small variability between equivalent cells (blue in Fig. 5C,E,G). From nullcline analysis of Eqns 1 and 2 in the absence of Dl1 and Atoh1, we extracted the minimal signaling strength to have bistability of homogeneous states:

$$\epsilon_{min}=\frac{\theta_z h_z (1+\beta_z \epsilon_r)^{1-1/h_z}}{\epsilon_r \beta_z (h_z-1)^{1-1/h_z}}. \quad (5)$$

Numerical integration of the dynamics

Simulation details

Numerical integration of the dynamics (Eqns 1-4) was performed with Runge-Kutta methods of the fourth order with time step 0.1 until the stationary state was reached, using a custom Fortran77 program (Fig. 5D-G and Fig. 6C; supplementary material Figs S5,S6,S8,S9). Supplementary material Simulation 1 is a Mathematica notebook [version 9.0, Wolfram Research; code provided in pdf and Mathematica notebook (.nb) format] also used for integration. Regular and irregular two-dimensional lattices of 12×12 or 18×18 cells with periodic boundary conditions were used. Irregularity parameter value was $\gamma=0.67$ (Formosa-Jordan et al., 2012). Initial condition for each molecular species x for the i-th cell was $x_i(t=0)=x_0(1+0.1U_i^x)$, with U_i^x being a uniform random number between -0.5 and 0.5 and x_0 a stationary homogeneous solution. LSA results were checked for different parameter values through numerical integration of the dynamics (data not shown).

Tissue state color representation

s_i, d_i, z_i and a_i values were represented in linear logarithmic grayscale. Cells with $s_i<0.1$, $d_i<1$, $z_i<0.1$ and $a_i<1$ were represented as white cells. Hair cells were defined as those expressing Atoh1 above a threshold and were represented in red. This threshold was the Atoh1 value at the stationary homogeneous state with intermediate Atoh1 level of the corresponding parameter values unless otherwise stated.

Pattern maintenance

We performed numerical integration of Eqns 1-4 on 3×3 perfectly hexagonal cells with periodic conditions and initial condition $x_i(t=0)=x_{pi}(1+0.1U_i^x)$, with U_i^x being defined as above and x_{pi} a stable fine-grained pattern solution. Pattern maintenance was considered to hold when the final state had between 20% and 80% of the cells in a high Atoh1 state (i.e. high Atoh1 levels were at least 1% higher than the minimal levels of Atoh1 in the same tissue).

Numerical simulations of electroporation

N_{EP} cells within a patch of N_P cells in a perfect hexagonal cellular array were randomly electroporated (fraction of electroporated cells=N_{EP}/N_P). Electroporation was performed at time $t_{EP}=49$ when the hair cell pattern had not yet formed. For gain of function, the exogenous electroporated Jag1 (z') had the dynamics:

$$\frac{dz_i'}{dt}=\nu_z'\{\beta_z'-z_i'\}, \quad (6)$$

with $\beta_z'=20\beta_z$ being its production and $\nu_z'=1$ its time-scale with respect to Notch degradation. Instead of Eqn 1, the Notch signal dynamics reads:

$$\frac{ds_i}{dt}=\frac{\epsilon\epsilon_r(\langle z_i\rangle+\langle z_i'\rangle)+\langle d_i\rangle}{1+\epsilon_r(\langle z_i\rangle+\langle z_i'\rangle)+\langle d_i\rangle}-s_i. \quad (7)$$

Integration of Eqns 2-4,6,7 was performed. Electroporated cells correspond to $\beta_z'=0$ for $t<t_{EP}$ and $\beta_z'=20\beta_z$ for $t\geq t_{EP}$ and $z_i'(t=0)=0$. Non-electroporated cells have $\beta_z'=0$. For loss of function, Eqns 1-4 were integrated with $\beta_z=0$ at $t_{EP}\geq49$ in electroporated cells. Bar charts show averages of the results and s.e.m. for three random patterns of electroporations. Control electroporations correspond to $\beta_z'=\beta_z$. Simulations assume a constant cell number, therefore, the potential effect of newly added cells was not considered.

Acknowledgements

This work is dedicated to the memory of Julian Lewis, whose work has been an example of scientific merit and a source of inspiration to the authors. We thank Domingos Henrique, Anna Bigas and Saúl Ares for critical reading of the manuscript, and Andrés Kamaid for kindly sharing results. LY411575 was made in the College of Life Sciences, Dundee University, and is a kind gift from Kim Dale. Warren Pear kindly provided NICD mutant constructs. We thank Marta Linares, Andreu Alibés and Miquel Sas for technical assistance.

Competing interests

The authors declare no competing financial interests.

Author contributions

Experimental work was performed by J.P., G.A., J.N. and F.G. Modeling was performed by P.F.-J., J.C.L.-E. and M.I.

Funding

The work was supported by grants from Ministerio de Ciencia e Innovacion (MICINN) [BFU-2011-24057, PLE-2009-0098, FIS2012-37655-C02-02] and Generalitat de Catalunya (GENCAT) [2009SGR14], Spain; fellowships SFRH/BPD/70691/2010 to J.N. from Fundação para a Ciência e a Tecnologia (FCT), Portugal; FPU-AP2008-03325 to P.F.-J. from Ministerio de Educación (MEC); and BES-2009-022286 to J.P. from MICINN, Spain.

Supplementary material

Supplementary material available online at
http://dev.biologists.org/lookup/suppl/doi:10.1242/dev.108100/-/DC1

References

Abelló, G., Khatri, S., Giráldez, F. and Alsina, B. (2007). Early regionalization of the otic placode and its regulation by the Notch signaling pathway. *Mech. Dev.* **124**, 631-645.

Acloque, H., Wilkinson, D. G. and Nieto, M. A. (2008). In situ hybridization analysis of chick embryos in whole-mount and tissue sections. *Methods Cell Biol.* **87**, 169-185.

Adam, J., Myat, A., Le Roux, I., Eddison, M., Henrique, D., Ish-Horowicz, D. and Lewis, J. (1998). Cell fate choices and the expression of Notch, Delta and Serrate homologues in the chick inner ear: parallels with Drosophila sense-organ development. *Development* **125**, 4645-4654.

Benedito, R., Roca, C., Sörensen, I., Adams, S., Gossler, A., Fruttiger, M. and Adams, R. H. (2009). The notch ligands Dll4 and Jagged1 have opposing effects on angiogenesis. *Cell* **137**, 1124-1135.

Bray, S. J. (2006). Notch signalling: a simple pathway becomes complex. *Nat. Rev. Mol. Cell Biol.* **7**, 678-689.

Brooker, R., Hozumi, K. and Lewis, J. (2006). Notch ligands with contrasting functions: Jagged1 and Delta1 in the mouse inner ear. *Development* **133**, 1277-1286.

Brückner, K., Perez, L., Clausen, H. and Cohen, S. (2000). Glycosyltransferase activity of Fringe modulates Notch-Delta interactions. *Nature* **406**, 411-415.
Buchler, N. E., Gerland, U. and Hwa, T. (2003). On schemes of combinatorial transcription logic. *Proc. Natl. Acad. Sci. U.S.A.* **100**, 5136-5141.
Chen, P. and Segil, N. (1999). p27(Kip1) links cell proliferation to morphogenesis in the developing organ of Corti. *Development* **126**, 1581-1590.
Chiang, M. Y., Xu, L., Shestova, O., Histen, G., L'Heureux, S., Romany, C., Childs, M. E., Gimotty, P. A., Aster, J. C. and Pear, W. S. (2008). Leukemia-associated NOTCH1 alleles are weak tumor initiators but accelerate K-ras-initiated leukemia. *J. Clin. Invest.* **118**, 3181-3194.
Chrysostomou, E., Gale, J. E. and Daudet, N. (2012). Delta-like 1 and lateral inhibition during hair cell formation in the chicken inner ear: evidence against cis-inhibition. *Development* **139**, 3764-3774.
Cole, L. K., Le Roux, I., Nunes, F., Laufer, E., Lewis, J. and Wu, D. K. (2000). Sensory organ generation in the chicken inner ear: contributions of bone morphogenetic protein 4, serrate1, and lunatic fringe. *J. Comp. Neurol.* **424**, 509-520.
Collier, J. R., Monk, N. A. M., Maini, P. K. and Lewis, J. H. (1996). Pattern formation by lateral inhibition with feedback: a mathematical model of delta-notch intercellular signalling. *J. Theor. Biol.* **183**, 429-446.
Daudet, N. and Lewis, J. (2005). Two contrasting roles for Notch activity in chick inner ear development: specification of prosensory patches and lateral inhibition of hair-cell differentiation. *Development* **132**, 541-551.
Daudet, N., Ariza-McNaughton, L. and Lewis, J. (2007). Notch signalling is needed to maintain, but not to initiate, the formation of prosensory patches in the chick inner ear. *Development* **134**, 2369-2378.
Doetzlhofer, A., Basch, M. L., Ohyama, T., Gessler, M., Groves, A. K. and Segil, N. (2009). Hey2 regulation by FGF provides a Notch-independent mechanism for maintaining pillar cell fate in the organ of Corti. *Dev. Cell* **16**, 58-69.
Driver, E. C., Sillers, L., Coate, T. M., Rose, M. F. and Kelley, M. W. (2013). The Atoh1-lineage gives rise to hair cells and supporting cells within the mammalian cochlea. *Dev. Biol.* **376**, 86-98.
Du, X., Li, W., Gao, X., West, M. B., Saltzman, W. M., Cheng, C. J., Stewart, C., Zheng, J., Cheng, W. and Kopke, R. D. (2013). Regeneration of mammalian cochlear and vestibular hair cells through Hes1/Hes5 modulation with siRNA. *Hear. Res.* **304**, 91-110.
Eddison, M., Le Roux, I. and Lewis, J. (2000). Notch signaling in the development of the inner ear: lessons from Drosophila. *Proc. Natl. Acad. Sci. U.S.A.* **97**, 11692-11699.
Ferjentsik, Z., Hayashi, S., Dale, J. K., Bessho, Y., Herreman, A., De Strooper, B., del Monte, G., de la Pompa, J. L. and Maroto, M. (2009). Notch is a critical component of the mouse somitogenesis oscillator and is essential for the formation of the somites. *PLoS Genet.* **5**, e1000662.
Fischer, A. and Gessler, M. (2007). Delta-Notch – and then? Protein interactions and proposed modes of repression by Hes and Hey bHLH factors. *Nucleic Acids Res.* **35**, 4583-4596.
Formosa-Jordan, P. and Ibañes, M. (2009). Diffusible ligand and lateral inhibition dynamics for pattern formation. *J. Stat. Mech.* **2009**, P03019.
Formosa-Jordan, P. and Ibañes, M. (2014). Competition in Notch signaling with cis enriches cell fate decisions. *PLoS ONE* **9**, p. e95744.
Formosa-Jordan, P., Ibañes, M., Ares, S. and Frade, J. M. (2012). Regulation of neuronal differentiation at the neurogenic wavefront. *Development* **139**, 2321-2329.
Golson, M. L., Le Lay, J., Gao, N., Brämswig, N., Loomes, K. M., Oakey, R., May, C. L., White, P. and Kaestner, K. H. (2009). Jagged1 is a competitive inhibitor of Notch signaling in the embryonic pancreas. *Mech. Dev.* **126**, 687-699.
Haddon, C., Jiang, Y. J., Smithers, L. and Lewis, J. (1998). Delta-Notch signalling and the patterning of sensory cell differentiation in the zebrafish ear: evidence from the mind bomb mutant. *Development* **125**, 4637-4644.
Haines, N. and Irvine, K. D. (2003). Glycosylation regulates Notch signalling. *Nat. Rev. Mol. Cell Biol.* **4**, 786-797.
Hansson, E. M., Teixeira, A. I., Gustafsson, M. V., Dohda, T., Chapman, G., Meletis, K., Muhr, J. and Lendahl, U. (2006). Recording Notch signaling in real time. *Dev. Neurosci.* **28**, 118-127.
Hartman, B. H., Reh, T. A. and Bermingham-McDonogh, O. (2010). Notch signaling specifies prosensory domains via lateral induction in the developing mammalian inner ear. *Proc. Natl. Acad. Sci. U.S.A.* **107**, 15792-15797.
Hayashi, T., Kokubo, H., Hartman, B. H., Ray, C. A., Reh, T. A. and Bermingham-McDonogh, O. (2008). Hesr1 and Hesr2 may act as early effectors of Notch signaling in the developing cochlea. *Dev. Biol.* **316**, 87-99.
Helms, A. W., Abney, A. L., Ben-Arie, N., Zoghbi, H. Y. and Johnson, J. E. (2000). Autoregulation and multiple enhancers control Math1 expression in the developing nervous system. *Development* **127**, 1185-1196.
Henrique, D., Adam, J., Myat, A., Chitnis, A., Lewis, J. and Ish-Horowicz, D. (1995). Expression of a Delta homologue in prospective neurons in the chick. *Nature* **375**, 787-790.
Iso, T., Kedes, L. and Hamamori, Y. (2003). HES and HERP families: multiple effectors of the Notch signaling pathway. *J. Cell. Physiol.* **194**, 237-255.
Jeffries, S., Robbins, D. J. and Capobianco, A. J. (2002). Characterization of a high-molecular-weight Notch complex in the nucleus of Notch(ic)-transformed RKE cells and in a human T-cell leukemia cell line. *Mol. Cell. Biol.* **22**, 3927-3941.
Kageyama, R., Niwa, Y., Shimojo, H., Kobayashi, T. and Ohtsuka, T. (2010). Ultradian oscillations in Notch signaling regulate dynamic biological events. *Curr. Top. Dev. Biol.* **92**, 311-331.
Kamaid, A., Neves, J. and Giraldez, F. (2010). Id gene regulation and function in the prosensory domains of the chicken inner ear: a link between Bmp signaling and Atoh1. *J. Neurosci.* **30**, 11426-11434.
Katoh, M. (2006). Notch ligand, JAG1, is evolutionarily conserved target of canonical WNT signaling pathway in progenitor cells. *Int. J. Mol. Med.* **17**, 681-685.
Kiernan, A. E., Cordes, R., Kopan, R., Gossler, A. and Gridley, T. (2005). The Notch ligands DLL1 and JAG2 act synergistically to regulate hair cell development in the mammalian inner ear. *Development* **132**, 4353-4362.
Kiernan, A. E., Xu, J. and Gridley, T. (2006). The Notch ligand JAG1 is required for sensory progenitor development in the mammalian inner ear. *PLoS Genet.* **2**, e4.
Le, T. T., Conley, K. W. and Brown, N. L. (2009). Jagged 1 is necessary for normal mouse lens formation. *Dev. Biol.* **328**, 118-126.
Li, S., Mark, S., Radde-Gallwitz, K., Schlisner, R., Chin, M. T. and Chen, P. (2008). Hey2 functions in parallel with Hes1 and Hes5 for mammalian auditory sensory organ development. *BMC Dev. Biol.* **8**, 20.
Liu, Z., Liu, Z., Walters, B. J., Owen, T., Kopan, R. and Zuo, J. (2013). In vivo visualization of Notch1 proteolysis reveals the heterogeneity of Notch1 signaling activity in the mouse cochlea. *PLoS ONE* **8**, e64903.
Matsuda, M., Koga, M., Nishida, E. and Ebisuya, M. (2012). Synthetic signal propagation through direct cell-cell interaction. *Sci. Signal.* **5**, ra31.
Mazzone, M., Selfors, L. M., Albeck, J., Overholtzer, M., Sale, S., Carroll, D. L., Pandya, D., Lu, Y., Mills, G. B., Aster, J. C. et al. (2010). Dose-dependent induction of distinct phenotypic responses to Notch pathway activation in mammary epithelial cells. *Proc. Natl. Acad. Sci. U.S.A.* **107**, 5012-5017.
Morrison, A., Hodgetts, C., Gossler, A., Hrabé de Angelis, M. and Lewis, J. (1999). Expression of Delta1 and Serrate1 (Jagged1) in the mouse inner ear. *Mech. Dev.* **84**, 169-172.
Morsli, H., Choo, D., Ryan, A., Johnson, R. and Wu, D. K. (1998). Development of the mouse inner ear and origin of its sensory organs. *J. Neurosci.* **18**, 3327-3335.
Mulvaney, J. and Dabdoub, A. (2012). Atoh1, an essential transcription factor in neurogenesis and intestinal and inner ear development: function, regulation, and context dependency. *J. Assoc. Res. Otolaryngol.* **13**, 281-293.
Murata, J., Ohtsuka, T., Tokunaga, A., Nishiike, S., Inohara, H., Okano, H. and Kageyama, R. (2009). Notch-Hes1 pathway contributes to the cochlear prosensory formation potentially through the transcriptional down-regulation of p27Kip1. *J. Neurosci. Res.* **87**, 3521-3534.
Murray, J. D. (2002). *Mathematical Biology: I. An Introduction*, Vol. 1, 3rd edn. p. 576. Berlin, Heidelberg: Springer-Verlag.
Neves, J., Kamaid, A., Alsina, B. and Giraldez, F. (2007). Differential expression of Sox2 and Sox3 in neuronal and sensory progenitors of the developing inner ear of the chick. *J. Comp. Neurol.* **503**, 487-500.
Neves, J., Parada, C., Chamizo, M. and Giraldez, F. (2011). Jagged 1 regulates the restriction of Sox2 expression in the developing chicken inner ear: a mechanism for sensory organ specification. *Development* **138**, 735-744.
Neves, J., Uchikawa, M., Bigas, A. and Giraldez, F. (2012). The prosensory function of Sox2 in the chicken inner ear relies on the direct regulation of Atoh1. *PLoS ONE* **7**, e30871.
Neves, J., Abelló, G., Petrovic, J. and Giraldez, F. (2013). Patterning and cell fate in the inner ear: a case for Notch in the chicken embryo. *Dev. Growth Differ.* **55**, 96-112.
Ninov, N., Borius, M. and Stainier, D. Y. R. (2012). Different levels of Notch signaling regulate quiescence, renewal and differentiation in pancreatic endocrine progenitors. *Development* **139**, 1557-1567.
Oesterle, E. C. and Rubel, E. W. (1993). Postnatal production of supporting cells in the chick cochlea. *Hear. Res.* **66**, 213-224.
Owen, M. R., Sherratt, J. A. and Wearing, H. J. (2000). Lateral induction by juxtacrine signaling is a new mechanism for pattern formation. *Dev. Biol.* **217**, 54-61.
Pan, W., Jin, Y., Stanger, B. and Kiernan, A. E. (2010). Notch signaling is required for the generation of hair cells and supporting cells in the mammalian inner ear. *Proc. Natl. Acad. Sci. U.S.A.* **107**, 15798-15803.
Perdigoto, C. N., Schweisguth, F. and Bardin, A. J. (2011). Distinct levels of Notch activity for commitment and terminal differentiation of stem cells in the adult fly intestine. *Development* **138**, 4585-4595.
Podgorski, G. J., Bansal, M. and Flann, N. S. (2007). Regular mosaic pattern development: a study of the interplay between lateral inhibition, apoptosis and differential adhesion. *Theor. Biol. Med. Model.* **4**, 43.
Pujades, C., Kamaid, A., Alsina, B. and Giraldez, F. (2006). BMP-signaling regulates the generation of hair-cells. *Dev. Biol.* **292**, 55-67.

Development (2014) 141, 2313-2324 doi:10.1242/dev.108100

Ramos, C., Rocha, S., Gaspar, C. and Henrique, D. (2010). Two Notch ligands, Dll1 and Jag1, are differently restricted in their range of action to control neurogenesis in the mammalian spinal cord. *PLoS ONE* **5**, e15515.

Robert-Moreno, A., Guiu, J., Ruiz-Herguido, C., López, M. E., Inglés-Esteve, J., Riera, L., Tipping, A., Enver, T., Dzierzak, E., Gridley, T. et al. (2008). Impaired embryonic haematopoiesis yet normal arterial development in the absence of the Notch ligand Jagged1. *EMBO J.* **27**, 1886-1895.

Savill, N. J. and Sherratt, J. A. (2003). Control of epidermal stem cell clusters by Notch-mediated lateral induction. *Dev. Biol.* **258**, 141-153.

Sprinzak, D., Lakhanpal, A., LeBon, L., Santat, L. A., Fontes, M. E., Anderson, G. A., Garcia-Ojalvo, J. and Elowitz, M. B. (2010). Cis-interactions between Notch and Delta generate mutually exclusive signalling states. *Nature* **465**, 86-90.

Takebayashi, S., Yamamoto, N., Yabe, D., Fukuda, H., Kojima, K., Ito, J. and Honjo, T. (2007). Multiple roles of Notch signaling in cochlear development. *Dev. Biol.* **307**, 165-178.

Tateya, T., Imayoshi, I., Tateya, I., Ito, J. and Kageyama, R. (2011). Cooperative functions of Hes/Hey genes in auditory hair cell and supporting cell development. *Dev. Biol.* **352**, 329-340.

Webb, S. D. and Owen, M. R. (2004). Oscillations and patterns in spatially discrete models for developmental intercellular signalling. *J. Math. Biol.* **48**, 444-476.

Zheng, J. L., Shou, J., Guillemot, F., Kageyama, R. and Gao, W. Q. (2000). Hes1 is a negative regulator of inner ear hair cell differentiation. *Development* **127**, 4551-4560.

Zine, A., Van De Water, T. R. and de Ribaupierre, F. (2000). Notch signaling regulates the pattern of auditory hair cell differentiation in mammals. *Development* **127**, 3373-3383.

Zine, A., Aubert, A., Qiu, J., Therianos, S., Guillemot, F., Kageyama, R. and de Ribaupierre, F. (2001). Hes1 and Hes5 activities are required for the normal development of the hair cells in the mammalian inner ear. *J. Neurosci.* **21**, 4712-4720.

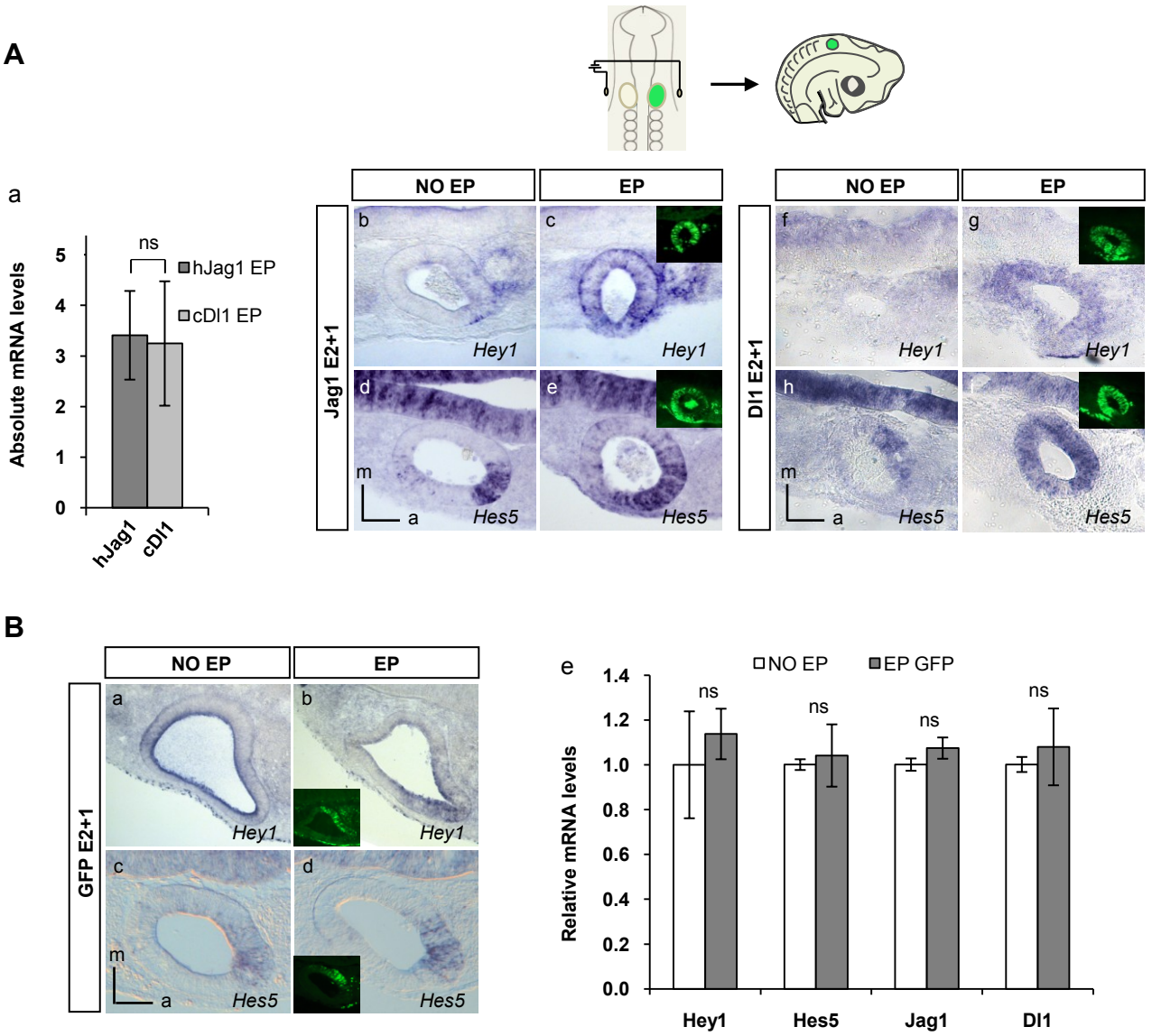

Figure S1. hJag1, cDl1 and GFP electroporations. (A) Absolute hJag1 and cDl1 mRNA levels ($2^{-\Delta Ct}$) 12h after hJag1 and cDl1 electroporation indicate that transfection levels are comparable. Values are mean ± s.e.m. of five independent experiments (a). Coronal sections of otic vesicles from chicken embryos that were electroporated at E2 with hJag1 (b-e) or cDl1 (f-i) and allowed to develop one day in ovo. The diagram on the top illustrates the procedure. Sections were developed by ISH for Hey1 (b-c, f-g) or Hes5 (d-e, h-i) and stained for GFP (inset, green). (B) The expression patterns of Hey1 (a-b) and Hes5 (c-d) were not altered by GFP electroporation. Similarly, Hey1, Hes5, Jag1 and Dl1 relative mRNA levels evaluated by qRT-PCR are not significantly changed in otic vesicles electroporated with GFP when compared to control (not electroporated) otic vesicles. Values are relative to control (not electroporated) otic vesicles and are mean ± s.e.m. of tree independent experiments (e). Statistical significance was tested by comparing ΔCts in Student's t-test.

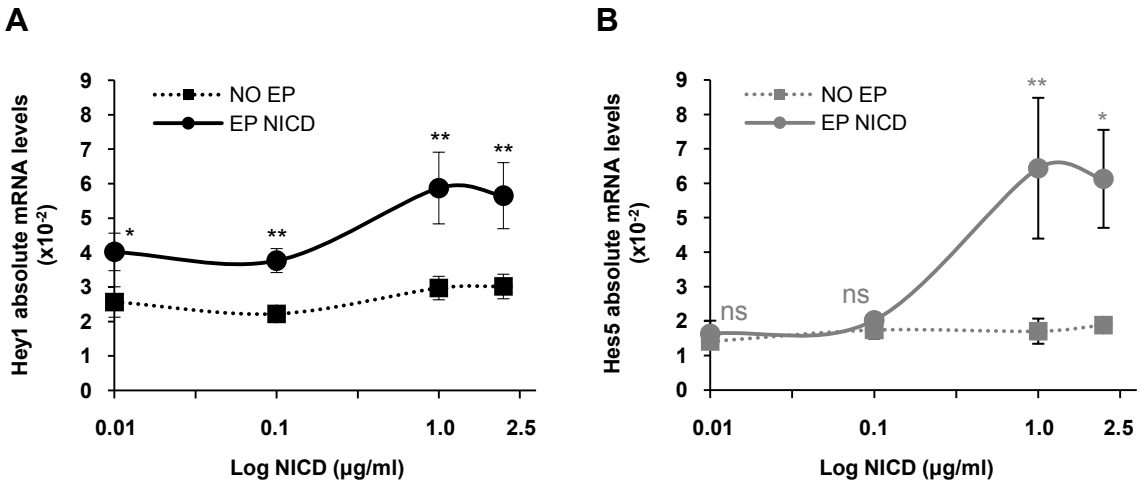

Figure S2. Hey1 and Hes5 are readouts of Notch signal strength. Absolute mRNA levels ($2^{-\Delta Ct}x10^{-2}$) of Hey1 (A, black dots and squares) and Hes5 (B, gray dots and squares) after electroporation at E2 with increasing concentrations of NICD and analysis one day after. Values are mean ± s.e.m. of duplicate analysis of n=4-5 independent experiments. Statistical significance was tested by comparing individual ΔCt from experimental and control (not electroporated) side from each experiment in Student's t-test.

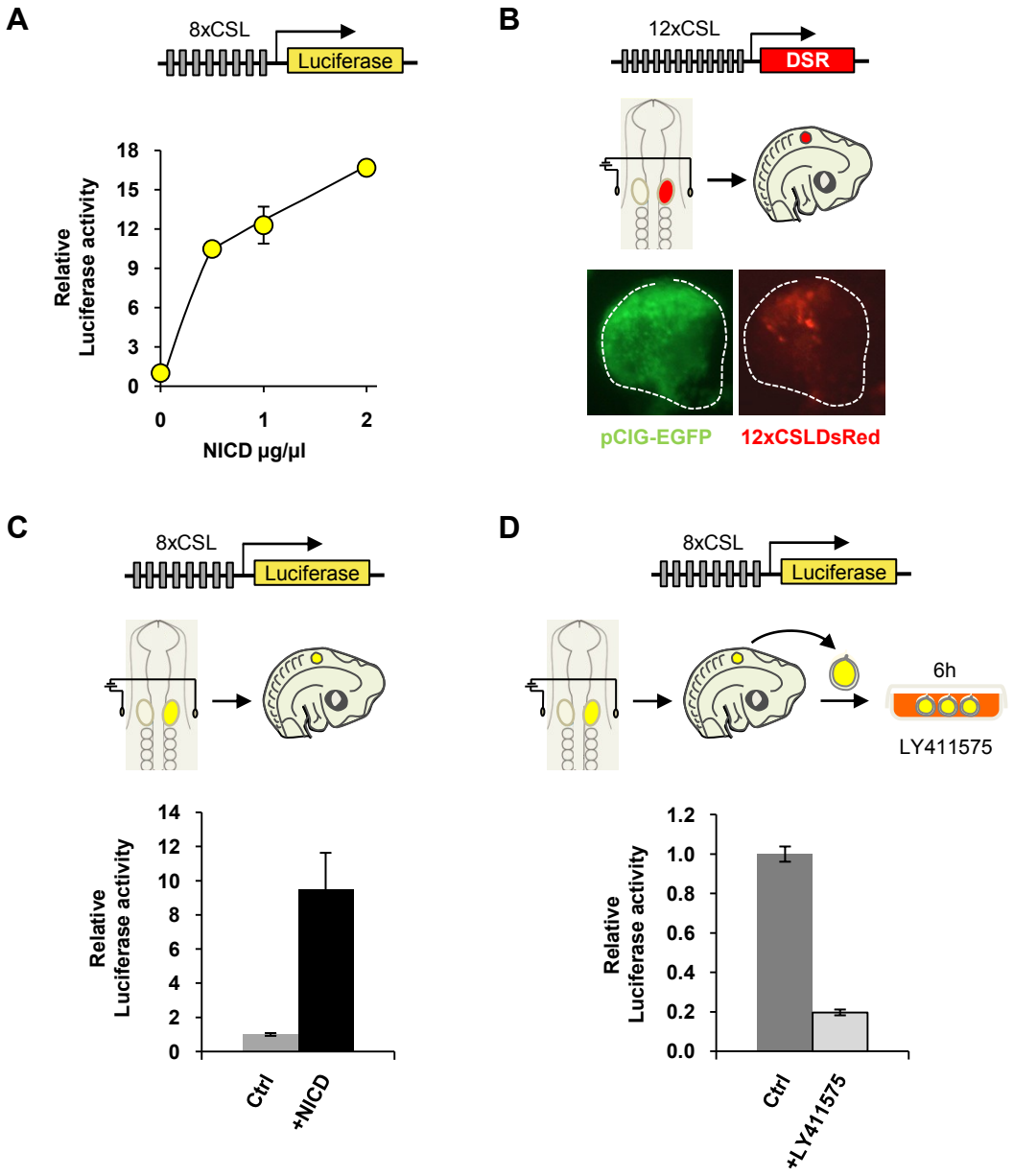

Figure S3. Quantification of the levels of Notch activity in the otic vesicle. (A) Relative Luciferase activity in HEK293T cells transfected with different levels of NICD. Luciferase expression is driven by 8 multimerized CSL binding sites and it is proportional to NICD levels. This experiment indicates that 8xCSL-Luc reporter is sensitive to different levels of NICD. (B) Direct DsRed expression in one otic vesicle electroporated with 12xCSL-DsRed (n=8). DsRed expression is driven by 12 multimerized CSL binding sites. This experiment indicates that endogenous Notch activity can be detected in the otic vesicle using this construct. (C) Relative Luciferase activity in otic vesicles electroporated with 1 µg/µl mNICD and 8xCSL-Luc from n=3 independent experiments. As with DsRed, endogenous Notch activity can be detected with 8xCSL-Luc reporter (light grey) and reporter activity is significantly increased by co-transfection with mNICD (black), indicating that also in vivo, this reporter responds to increased concentration of NICD. (D) Relative Luciferase activity in otic vesicles electroporated with 8xCSL-Luc and cultured in the presence of LY411575 for 6h, relative to otic vesicles cultured without inhibitor. This experiment indicates that the levels of Notch activity measured by Luciferase reporter activity decay after addition of LY411575 to the culture medium.

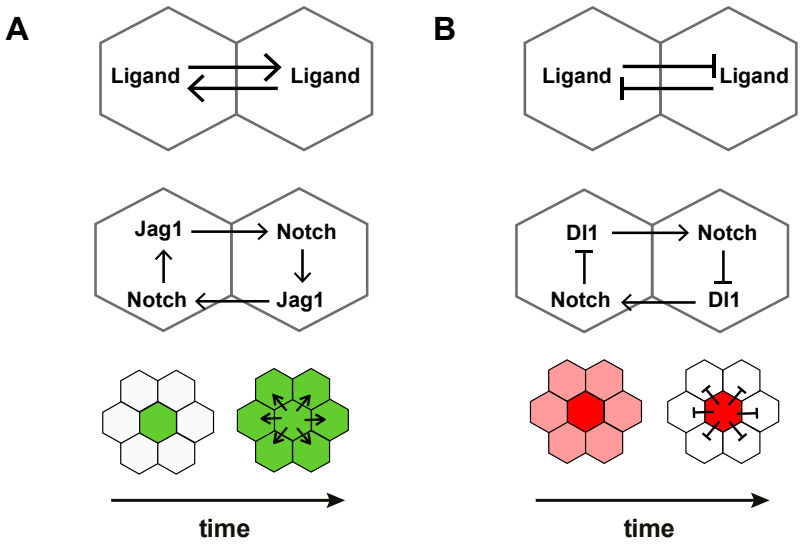

Figure S4. Lateral induction drives ligand propagation, while lateral inhibition generates fine-grained patterning. (A) Lateral induction and (B) lateral inhibition circuits and its patterning effects. Top: mutual activation and mutual inhibition feedback loops between two equivalent adjacent cells. Middle: The circuit on the top is detailed for Notch signaling driven by a single ligand (Jag1 for A and Dl1 for B). Jag1 is activated by Notch, while Dl1 is inhibited by Notch. Bottom: Lateral induction and lateral inhibition of ligand occurring when a central cell expresses the ligand strongly (green for Jag1 and red for Dl1).

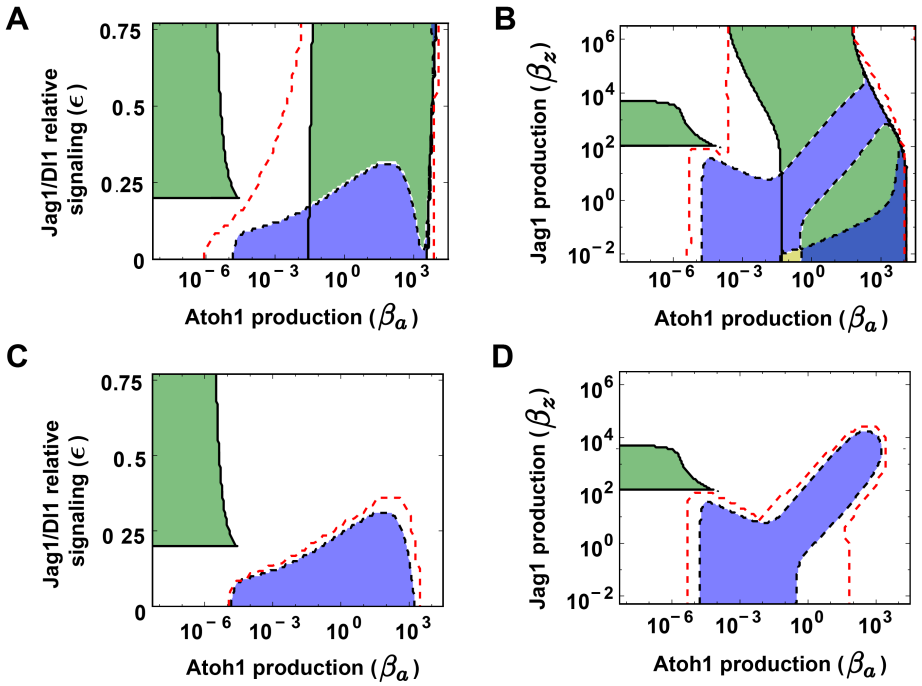

Figure S5. The absence of Atoh1 autoactivation reduces pattern maintenance capabilities. (A, B) correspond to panels 5E and 5G (middle) where additional regions with two stable homogeneous states (green at high β_a, yellow and dark blue) computed from LSA (Methods and see below) are shown. These regions have been omitted in Fig. 5 for the sake of simplicity and comprehension of the figure since they do not inform about the prosensory or hair cell pattern formation regions. We include them here for completitude. (C, D) Panels A and B without the Atoh1 autoactivation loop ($\alpha = 0$). In all panels, dashed red lines indicate pattern maintenance as in Fig. 5. In the absence of Atoh1 autoactivation, pattern maintenance regions are greatly reduced, as well as bistable regions for high Atoh1 productions. In contrast, pattern formation regions (light blue) remain nearly unchanged. Parameter values in all panels are as detailed in Materials and Methods. In all panels we used $h_d = 1, h_{a1} = h_z = 4$. For $\alpha = 0$, this drives the same effective cooperativity of Dl1 on Notch1 signaling ($h_d h_{a1} = 4$) as Jag1 has ($h_z = 4$). Results depicted in all panels corresponds to linear stability analysis (LSA, Materials and Methods). LSA as explained in Materials and Methods resulted in the following Routh-Hurwitz conditions (Murray, 2002):

$$q_1 > 0 \qquad \text{(S1)}$$

$$q_1 q_2(\Omega) - q_3(\Omega) > 0 \qquad \text{(S2)}$$

$$q_1 q_2(\Omega) q_3(\Omega) - q_3^2(\Omega) - q_1^2(\Omega) q_4(\Omega) > 0 \qquad \text{(S3)}$$

$$q_4(\Omega) > 0, \qquad \text{(S4)}$$

with

$$q_1 = 1 + v_d + v_z - R_{aa} \,,$$

$$q_2(\Omega) = v_d + (1 + v_d) v_z - (1 + v_d + v_z) R_{aa} - \Omega A_z R_{zs} \,,$$

$$q_3(\Omega) = v_d v_z - \big(v_z + v_d(1+v_z)\big) R_{aa} - \Omega A_d R_{as} R_{da} + \Omega A_z (R_{aa} - v_d) R_{zs}$$

$$q_4(\Omega) = v_d R_{aa} (\Omega A_z R_{zs} - v_z) - v_z \Omega A_d R_{as} R_{da}$$

where $R_{xy} \equiv \frac{\partial}{\partial y_i}\left(\frac{dx_i}{dt}\right)\Big|_{homo}$ and $A_x \equiv \omega \frac{\partial}{\partial x_j}\left(\frac{ds_i}{dt}\right)\Big|_{homo}$. In these definitions, *homo* represents the homogeneous stationary state whose stability is evaluated, x and y stand for the model variables, the index j refers to a cell that is neighboring cell i, and ω is the number of first neighbors. Ω is a parameter that takes discrete values within the interval $\Omega \in [-0.5,1]$ and that accounts for different periodic perturbations of the hexagonal lattice (Formosa-Jordan and Ibañes, 2009). $\Omega = -0.5$ refers to the periodicity characteristic of lateral inhibition patterning, while $\Omega = 1$ refers to a homogeneous perturbation. Green regions correspond to parameter regions where two homogeneous solutions are stable and therefore satisfy inequalities S1-S4 for all Ω values. Light blue regions correspond to those parameter regions where at least one of the conditions S1-S4 is violated for $\Omega = -0.5$ and not $\Omega = 1$ (*i.e.* unstable to $\Omega = -0.5$ and stable to $\Omega = 1$). In these regions and according to the LSA (notice that $\Omega = -0.5$ is the perturbation that grows the fastest) the lateral inhibition pattern can emerge. These have been plotted in Fig. 5. The dark blue region in B corresponds to two homogeneous solutions stable to all Ω, plus another homogeneous solution unstable to all Ω with the fastest growing mode at $\Omega = -0.5$. This drives an irregular non periodic pattern. The yellow region in B has one homogeneous solution unstable to all Ω with the fastest growing mode at $\Omega = -0.5$ (*i.e.* an irregular non periodic pattern can emerge from this state), one homogeneous state stable to all Ω and one homogeneous state unstable to $\Omega = -0.5$ but not to $\Omega = 1$ (*i.e.* a periodic pattern can emerge from this other state).

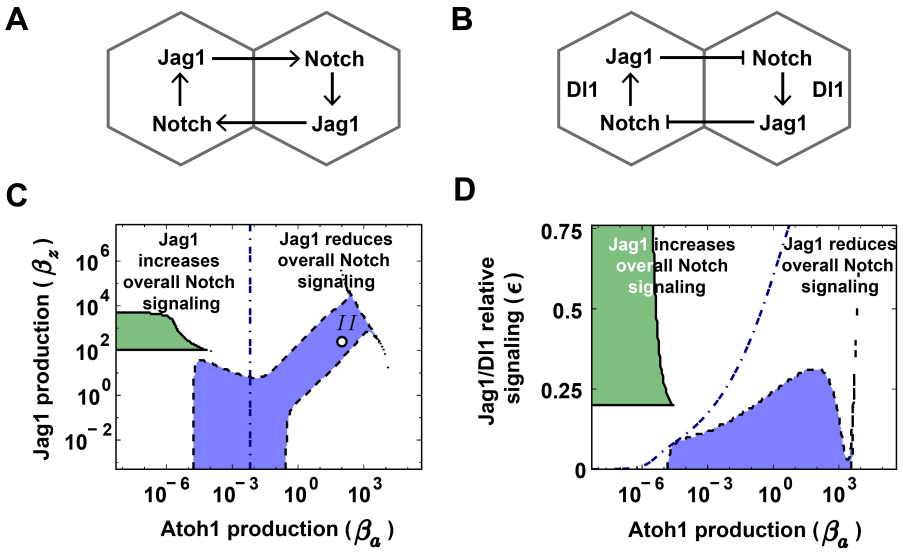

Figure S6. Jag1 switches its role when Dl1 arises. (A, B) Cartoons of interactions through Jag1 that are obtained from the model in Fig. 5B for equivalent cells. (A) In the absence of Dl1, Jag1 increases (arrow from cell to cell) the overall signal in an adjacent cell. Thus, the lateral induction module of Fig. S4A holds. (B) When there is enough Dl1 expressed, which signals with more strength than Jag1, Jag1 decreases the overall signal in the adjacent cell (blunt arrow from cell to cell). This decrease occurs because of competition between Dl1 and Jag1 for common resources of Notch signaling (Fig. 4). The cartoon shows that the regulatory interactions mediated by Jag1 ultimately drive mutual Jag1 inhibition between cells and therefore constitute a novel type of lateral inhibition. The interactions mediated by Dl1, which correspond to those in Fig. S4B, are not included for simplicity. Note that the arrow and the blunt arrow between cells in A and B stand only for the net effect of Jag1 on Notch signal, which depends on the amount of competition. (C,D) Regions where Jag1 increases or decreases overall Notch signaling within the phase diagrams of Fig. 5E and 5G (middle) respectively. The blue dot-dashed line divides the space in these two regions. Hence, this line divides the parameter space in a region where Jag1 drives lateral induction as in A (left regions) and another region (right ones) where Jag1 drives the type of lateral inhibition as in B. This line is defined by $\frac{\partial}{\partial <z_i>}\left(\frac{ds_i}{dt}\right)\Big|_{homo} = 0$ where the derivative is computed at the homogeneous stationary state of the dynamics of Eqns 1-4 (at the low Jag1 homogeneous state when multiple homogeneous states are present for high β_a, which has similar Jag1 values as the high Jag1 state of the prosensory). Hence, the derivative is evaluated on equivalent cells that express Jag1 and Dl1 (Dl1 is expressed at low values compared to those in hair cells), mimicking the equivalence of cells at the prosensory state before hair cell patterning is set. Point II corresponds to fine-grained patterning (blue) arising when Jag1 production decreases overall Notch signaling and hence it is performing the type of lateral inhibition of panel B. D shows that fine-grained patterning for high Jag1 production ($\beta_z = 250$) occurs when Jag1 reduces overall Notch signaling (*i.e.* drives mutual inhibition between adjacent cells).

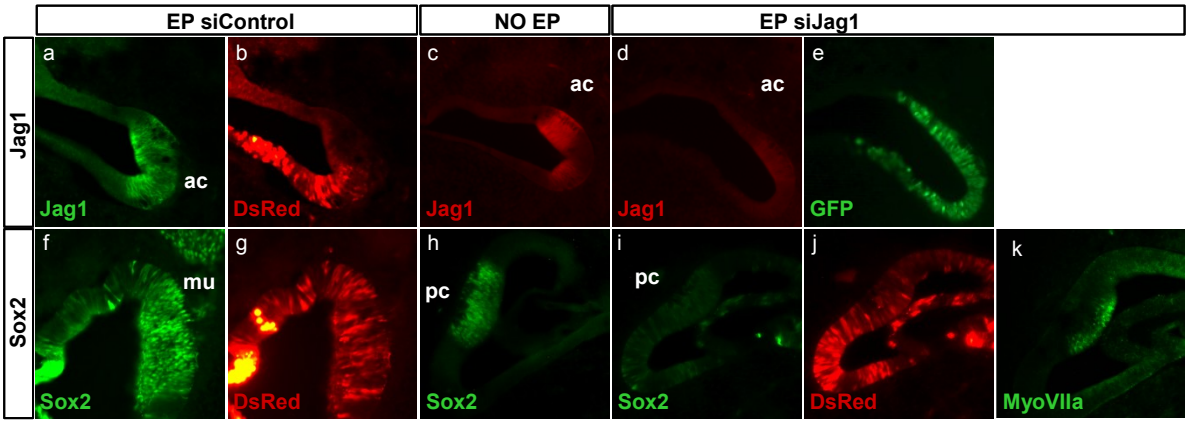

Figure S7. Stealth Jag1 downregulates Jag1 and Sox2 expression. Unaffected Jag1 expression after stealth control electroporation at E3.5+1 (a-b). Decreased Jag1 expression in stealth Jag1 electroporated crista at E3.5+2 (d-e) compared to non electroporated control (c). Unaffected Sox2 immunostaining after stealth control electroporation at E3.5+3 (f-g). Sox2 immunostaining of non electroporated (h), stealth Jag1 electroporated patch (i-j) and MyoVIIa immunostaining after stealth Jag1 electroporated patch at E3.5+3 in alternate section (k). DsRed and GFP were used as tracers for electroporation.

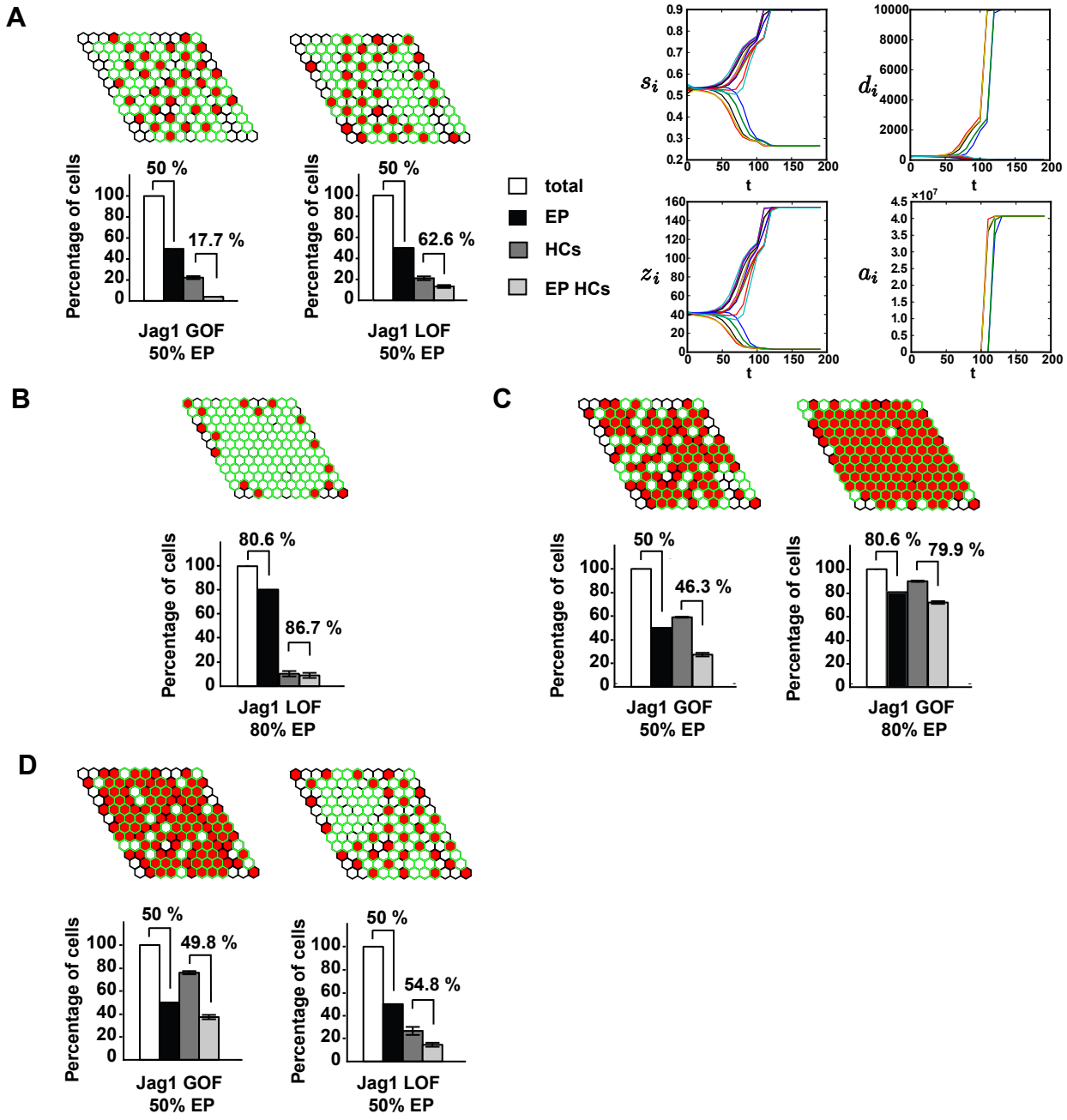

Figure S8. Numerical simulations of Jag1 gain of function (GOF) and loss of function (LOF) at different conditions. Hair cell (red) pattern at final simulation times and bar diagrams as in Fig. 6C. Each panel corresponds to a different condition which differs only in a single parameter value from the conditions of Fig. 6C: (A) GOF and LOF performed at earlier times (t_{EP}=0), (B) LOF with higher (80%) electroporation density, (C) GOF with higher exogenous Jag1 electroporation levels (β'_z=50β_z), (D) GOF and LOF with higher endogenous production rates (β_z=1000). (A, left) Time evolution of each variable in different cells (each line corresponds to a different cell) for point II in Fig. 5E for CTL electroporations. The pattern is not formed at t=t_{EP}=0 nor at t=t_{EP}=49. In all panels we used the color codes as in Fig. 6C. The threshold level of Atoh1 above which cells are considered hair cells is the same for all cells, being electroporated or not, as done in Fig. 6C, and was computed as described in Materials and Methods. Accordingly, this threshold level is the same in panels A-C and in Fig. 6C (threshold level: 2.629). Panel D has a different threshold level, defined by its parameter values (threshold level: 2.033). All patterns have been simulated with the same seed of random numbers for the initial condition that chooses which cells are electroporated. Therefore, all the snapshots that have the same percentage of electroporation have identical patterns of electroporated cells (green cell borders). Bar diagrams are averages and s.e.m. over three different set of random numbers (*i.e.* patterns of electroporation).

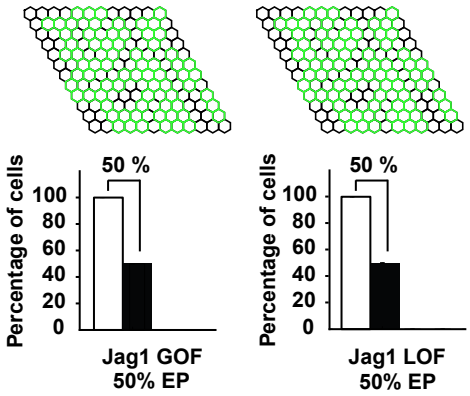

Figure S9. Atoh1 autoactivation drives robustness to patterning. Numerical simulation of gain of function (GOF) and loss of function (LOF) as in Fig. 6C but in the absence of Atoh1 autoactivation (*α=0*). Patterning is disrupted. Hair cells are defined at the same threshold level of Atoh1 as in Fig. 6C. All other parameter values and conditions as in Fig. 6C. The same identical patterns of electroporation (green cell borders) have been used in both panels (as in Fig. S8 for the same percentage of electroporation). Despite the signal, ligands and Atoh1 activities driven by GOF and LOF are different (data not shown), they all result in the absence of HCs. Therefore, both patterns look identical. Bar diagrams are averages and s.e.m. over three different set of random numbers (i.e. patterns of electroporation).

Movie 1. Dynamics of ligand propagation through lateral induction. *In silico* dynamics of (left) Dl1 and (right) Jag1 corresponding to Fig. 5D.

Movie 2. Dynamics of fine grained pattern formation through lateral inhibition. *In silico* dynamics of (left) Dl1 and (right) Jag1 corresponding to Fig. 5F. Plots of these dynamics in different cells are shown in Fig. S8A.

Simulation 1. Code for simulating ligand propagation and fine-grained patterning for the model with two ligands regulated oppositely by Notch. Mathematica notebook that integrates Eqns (1-4) on a perfect hexagonal lattice with periodic boundary conditions and represents the results on a regular hexagonal cellular lattice. Homogeneous initial conditions with small perturbations are used as explained in Methods. A local perturbation can be also included in the initial conditions for driving ligand propagation in the appropriate lateral induction regions. The code runs properly in both Mathematica 8.0 and 9.0 software.

Download Simulation 1. PDF

Download Simulation 1. Code

Table S1. Stealth Jag1 RNAi and stealth control duplex oligonucleotide sequences

siRNA	si RNA sequence1	siRNA sequence2 (reverse complement)
si_Jag1 #1	CCUUGUGAAGUAAUCGACAGCUGUA	UACAGCUGUCGAUUACUUCACAAGG
si_Jag1#2	AUUGCAUGUUGCCUCAUCACACUGG	CCAGUGUGAUGAGGCAACAUGCAAU
si_Jag1#3	CGGAGCAAAUACUGUUCCAAUUAAA	UUUAAUUGGAACAGUAUUUGCUCCG
si_ctrl #1	CCUAAGUAAUGAGCUCGACUGUGUA	UACACAGUCGAGCUCAUUACUUAGG
si_ctrl #2	AUUCAGACGUUUCGUCACCUCAUGG	CCAUGAGGUGACGAAACGUCUGAAU
st_ctrl #3	CGGAACAUAGUCCUUAACUUAGAAA	UUUCUAAGUUAAGGACUAUGUUCCG

Table S2. qRT-PCR primer sequences

Gene	Forward primer	Reverse primer
GAPDH	TTGGCATTGTGGAGGGTCTT	GTGGACGCTGGGATGATGTT
cHey1	CGGAGGGAAAGGTTATTTCG	CAGCAATGGGTGAGATATGTG
cHes5	GAAATCCTGACACCCAAAGAG	TCAATGCTGCTGTTAATCCT
cDl1	TTGACCTGGGGAACTCCTAC	GGTGCAGGAGTAGTCGTTGA
cJag1	TGCCAGACGGTGCTAAGTG	TCGAGGACCACACCAAACC
hJag1	CAACCGTGCCAGTGACTATTTCTGC	TGTTCCCGTGAAGCCTTTGTTACAG
DSR	CCAAGCTGAAGGTGACCAAG	CCGTCCTCGAAGTTCATCAC

Gapdh was used as calibrator gene.